OFFICE OF NAVAL RESEARCH

Contract N7onr-35301

T. O. I.

NR-041-032

Technical Report No. 107

THE EFFECT OF SHEAR STRESSES ON THE CARRYING CAPACITY OF I-BEAMS

by

C.-F. A. Leth

GRADUATE DIVISION OF APPLIED MATHEMATICS

BROWN UNIVERSITY

PROVIDENCE, R. I.

March, 1954

APPROVED DISTRIBUTION LIST FOR UNCLASSIFIED TECHNICAL REPORTS
Issued by
BROWN UNIVERSITY
Contract N7onr-358, T.O. 1
NR 041 032

Office of Naval Research
Washington 25, D. C.

M-2	Attn: Mathematics Branch (Code 432)
M-1	Mechanics Branch (Code 438)
M-1	Physics Branch (Code 421)
M-1	Metallurgy Branch (Code 423)

M-2 Commanding Officer
Office of Naval Research Branch Office
150 Causeway Street
Boston, Massachusetts

M-1 Commanding Officer
Office of Naval Research Branch Office
346 Broadway
New York, New York

M-1 Commanding Officer
Office of Naval Research Branch Office
844 North Rush Street
Chicago 11, Illinois

M-1 Commanding Officer
Office of Naval Research Branch Office
1000 Geary Street
San Francisco 9, California

M-1 Commanding Officer
Office of Naval Research Branch Office
1030 East Green Street
Pasadena 1, California

M-18 Officer-in-Charge
Office of Naval Research
Navy #100
Fleet Post Office
New York, New York

M-9 Director
Naval Research Laboratory
Washington 20, D. C.

	Attn: Scientific Information Division
M-2	Library (Code 2021)
M-1	Applied Mathematics Branch (Code 3830)
M-1	Shock and Vibrations Section (Code 3850)
M-1	Structures Branch (Code 3860)

Bureau of Ships
Department of the Navy
Washington 25, D. C.

M-2 Attn: Code 364 (Technical Library)
R-1 Code 423 (Underwater Explosion Research)
M-1 Code 442 (Scientific Section, Design)

David Taylor Model Basin
Carderock, Maryland

M-2 Attn: Library
M-1 Structural Mechanics Division

Naval Ordnance Laboratory
White Oak, Silver Spring 19, Maryland

M-2 Attn: Library

Bureau of Aeronautics
Department of the Navy
Washington 25, D. C.

M-1 Attn: AER-TD-414
R-1 Materials Branch
R-1 Design Elements Division

Bureau of Yards and Docks
Department of the Navy
Washington 25, D. C.

R-2 Attn: Director, Research Division

Commander
Norfolk Naval Shipyard
Norfolk, Virginia

M-1 Attn: Technical Library (Code 243A)
M-1 UERD (Code 290)

Superintendent
Aeronautical Structures Laboratory
Building 600, Naval Air Experimental Station
Philadelphia 12, Pennsylvania

R-1 Attn: Experimental Structures Section

Office, Assistant Chief of Staff, G4
The Pentagon
Washington, D. C.

M-1 Attn: Research and Development Division

M-1 The Chief, Armed Forces Special Weapons Project
Department of Defense
P. O. Box 2610
Washington, D. C.

U. S. Army Arsenal
Watertown 72, Massachusetts

M-1 Attn: Dr. R. Beeuwkes
M-1 Mr. J. Bluhm

Frankford Arsenal
Pitman-Dunn Laboratory
Philadelphia 37, Pennsylvania
M-1 Attn: Dr. Herbert I. Fusfeld

Picatinny Arsenal
Dover, New Jersey
M-1 Attn: Dr. L. Gilman

Commanding General
Wright Air Development Center
Wright-Patterson Air Force Base
Dayton, Ohio
M-4 Attn: WCACD

Department of Commerce
Office of Technical Service
Washington 25, D. C.
M-1 Attn: Library Section

National Advisory Committee for Aeronautics
1724 F. Street NW
Washington 25, D. C.
M-1 Attn: Chief of Aeronautical Intelligence

National Advisory Committee for Aeronautics
Langley Aeronautical Laboratory
Langley Field, Virginia
M-1 Attn: Library

National Advisory Committee for Aeronautics
Lewis Flight Propulsion Laboratory
Cleveland Airport
Cleveland 11, Ohio
M-1 Attn: Library

National Bureau of Standards
Washington, D. C.
M-1 Attn: Dr. W. R. Ramberg

Director of Research
Sandia Corporation
Albuquerque, New Mexico
M-1 Attn: Dr. S. C. Hight

Brooklyn Polytechnic Institute
85 Livingston Street
Brooklyn, New York
R-1 Attn: Dr. N. J. Hoff
R-1 Dr. H. Reissner
M-1 Dr. P. G. Hodge, Jr.
M-1 Dr. F. S. Shaw (Dept. Aero. Engr. & Appl. Mech.)

Brown University
Providence 12, Rhode Island
M-1 Attn: Chairman, Graduate Division of Applied Mathematics

California Institute of Technology
Pasadena, California

R-1 Attn: Dr. J. G. Kirkwood
R-1 Dr. Pol Duwez
R-1 Dr. H. S. Tsien

University of California
Berkeley, California

M-1 Attn: Dr. J. E. Dorn
R-1 Dr. H. Hultgren
R-1 Dr. G. C. Evans
M-1 Dr. C. F. Garland

University of California
Los Angeles, California

R-1 Attn: Dr. I. S. Sokolnikoff
R-1 Dr. D. Rosenthal

Carnegie Institute of Technology
Pittsburgh, Pennsylvania

R-1 Attn: Dr. J. S. Koehler
R-1 Dr. G. H. Handelman
M-1 Dr. E. Saibel
R-1 Dr. H. J. Greenberg
R-1 Dr. E. D'Appolonia

Case Institute of Technology
Cleveland, Ohio

M-1 Attn: Dr. W. M. Baldwin, Jr., Metals Research Laboratory
R-1 Dr. O. Hoffman

Catholic University of America
Washington, D. C.

M-1 Attn: Dr. F. A. Biberstein
R-1 Dr. K. Hertzfeld

University of Chicago
Chicago, Illinois

R-1 Attn: Dr. C. S. Barrett

Columbia University
New York, New York

M-1 Attn: Dr. R. D. Mindlin
M-1 Dr. H. Bleich
M-1 Dr. B. A. Boley
R-1 Dr. M. Gensamer

Cornell University
Ithaca, New York

R-1 Attn: Dr. H. S. Sack
R-1 Dr. A Kantrowitz

University of Florida
Gainesville, Florida

M-1 Attn: Dr. C. G. Smith

Harvard University
Cambridge 38, Massachusetts
R-1 Attn: Dr. F. Birch, Dunbar Laboratory
M-1 Dr. George F. Carrier, 309 Pierce Hall

Illinois Institute of Technology
Chicago, Illinois
R-1 Attn: Dr. L. H. Donnell
M-1 Dr. E. Sternberg
R-1 Dr. W. Osgood

University of Illinois
Urbana, Illinois
M-1 Attn: Dr. N. M. Newmark
R-1 Engineering
R-1 T. J. Dolan
R-1 Dr. F. Seitz, Department of Physics
M-1 Department of Theoretical and Applied Mathematics, Attn: Prof. M. C. Steele

Indiana University
Bloomington, Indiana
M-1 Attn: Dr. T. Y. Thomas

Institute for Advanced Study
Princeton, New Jersey
R-1 Attn: Dr. J. von Neumann

Iowa State College
Ames, Iowa
R-1 Attn: Dr. G. Murphy
R-1 Dr. D. L. Holl

Johns Hopkins University
Baltimore, Maryland
M-1 Attn: Dr. W. H. Hoppman, II

M-1 Director, Applied Physics Laboratory
Johns Hopkins University
8621 Georgia Avenue
Silver Spring, Maryland

Lehigh University
Bethlehem, Pennsylvania
R-1 Attn: Mr. Lynn S. Beedle

Massachusetts Institute of Technology
Cambridge 39, Massachusetts
R-1 Attn: Dr. F. B. Hildebrand
R-1 Dr. J. M. Lessels
R-1 Dr. W. M. Murray
R-1 Dr. E. Reissner
R-1 Dr. M. Cohen, Rm. 8-413, Dept. of Metallurgy
R-1 Dr. B. L. Averbach, Department of Metallurgy
R-1 Dr. J. T. Norton
R-1 Dr. E. Orowan
M-1 Dr. R. Bisplinghoff, Dept. Aero. Engr.

University of Michigan
Ann Arbor, Michigan
M-1 Attn: Dr. Bruce G. Johnston
M-1 Dr. Paul Nagdhi, Dept. of Engineering Mechanics
R-1 Dr. N. Coburn
R-1 Dr. W. Kaplan

New York University
Institute for Mathematics & Mechanics
45 Fourth Avenue
New York 3, New York
R-1 Attn: Professor R. Courant
R-1 Dr. G. Hudson

New York University
New York 53, New York
R-1 Attn: Dr. C. T. Wang, Dept. of Aeronautics

Northwestern University
Evanston, Illinois
R-1 Attn: Dr. M. M. Hetenyi

University of Notre Dame
Notre Dame, Indiana
R-1 Attn: Dr. P. A. Beck

Pennsylvania State College
State College, Pennsylvania
R-1 Attn: Dr. J. A. Sauer
R-1 Dr. Joseph Marin
R-1 Dr. J. W. Fredrickson

Princeton University
Princeton, New Jersey
R-1 Attn: Dr. S. Lefschetz
R-1 Dr. L. Lees
R-1 Dr. J. V. Charyk

Purdue University
Lafayette, Indiana
M-1 Attn: Dr. C. A. Eringen

Rensselaer Polytechnic Institute
Troy, New York
R-1 Attn: Library
R-1 Dr. Paul Leiber
R-1 Dr. C. O. Dohrenwend
R-1 Dr. G. H. Lee

Santa Clara University
Santa Clara, California
M-1 Attn: Dr. R. M. Hermes

Stanford University
Stanford, California
R-1 Attn: Dr. L. Jacobsen
M-1 Dr. A. Phillips, Dept. of Mechanical Engineering
R-1 Dr. J. N. Goodier

Stevens Institute of Technology
Hoboken, New Jersey
R-1 Attn: Dr. E. G. Schneider

Swarthmore College
Swarthmore, Pennsylvania
M-1 Attn: Capt. W. P. Roop
R-1 Dr. S. T. Carpenter

University of Texas
Austin 12, Texas
R-1 Attn: Dr. A. A. Topractsoglou

University of Utah
Salt Lake City, Utah
M-1 Attn: Dr. H. Eyring

Washington State College
Pullman, Washington
R-1 Attn: Dr. B. Fried

Wheaton College
Norton, Massachusetts
R-1 Attn: Dr. H. Geiringer

Aerojet, Inc.
Azusa, California
R-1 Attn: F. Zwicky

Aluminum Company of America
New Kensington, Pennsylvania
M-1 Attn: R. L. Templin
M-1 H. N. Hill, Aluminum Research Laboratory

Armstrong Cork Company
Lancaster, Pennsylvania
R-1 Attn: J. W. Scott

Bell Telephone Laboratories
Murray Hill, New Jersey
R-1 Attn: C. Herring
R-1 D. P. Ling
R-1 W. P. Mason

Corning Glass Company
Corning, New York
R-1 Attn: J. T. Littleton

E. I. Dupont de Nemours & Co., Inc.
Wilmington 98, Delaware
R-1 Attn: J. H. Faupel, Materials of Construction Section

General Electric Company
Schenectady, New York
R-1 Attn: H. Fehr
R-1 H. Poritsky
R-1 J. H. Hollomon

General Motors
Detroit, Michigan
R-1 Attn: J. O. Almen

Lockheed Aircraft Company
Department 72-25, Factory A-1, Building 66
Burbank, California
R-1 Attn: Engineering Library

Midwest Research Institute
Kansas City, Missouri
R-1 Attn: M. Goland

Pratt & Whitney Aircraft Corporation
East Hartford, Connecticut
R-1 Attn: R. Morrison

U. S. Rubber Company
Passaic, New Jersey
R-1 Attn: H. Smallwood

Welding Research Council
Engineering Foundation
29 West 39 Street
New York 18, New York
M-1 Attn: W. Spraragen, Director

Westinghouse Research Laboratories
East Pittsburgh, Pennsylvania
R-1 Attn: Dr. E. A. Davis

M-1 Dr. A. Nadai
136 Cherry Valley Road
Pittsburgh 21, Pennsylvania

Westinghouse Electric Corporation
Lester Branch P.O.
Philadelphia, Pennsylvania
R-1 Attn: R. P. Kroon, Manager of Engineering, AGT Division

University of Pennsylvania
Towne Scientific School
Philadelphia 4, Pennsylvania
R-1 Attn: Dr. C. W. MacGregor, Vice President in Charge of Scientific and Engineering Studies

R-1 Professor G. Wästlund
Cement & Concrete Research Institute
Royal Institute of Technology
Stockholm 70, SWEDEN

M-1 Professor John E. Goldberg
Department of Structural Engineering
Purdue University
Lafayette, Indiana

R-1 Milad F. Hanna
% F.S.S.B.
Massachusetts Institute of Technology
Cambridge 39, Massachusetts

R-1 Dr. W. Freiberger
Department of Supply
Aeronautical Research Laboratories
Box 4331 GPO
Melbourne, AUSTRALIA

M-1 Professor B. W. Shaffer
Department of Mechanical Engineering
New York University
New York 53, New York

M-1 Professor G. Sachs
Division of Metallurgical Research
Engineering & Science Campus
East Syracuse 4, N. Y.

R-1 Professor Aziz Ghali
Head, Structural Analysis Department
Fonad University
Giza, EGYPT

M-1 Professor Hugh Ford
Mechanical Engineering Department
Imperial College of Science & Technology
London, S.W.7
ENGLAND

R-1 Dr. R. H. Wood
D.S.I.R. Building Research Station
Garston, Watford, Herts
ENGLAND

ACKNOWLEDGEMENT

The author wishes to express his sincere gratitude to Professor P. S. Symonds for his many valuable suggestions and his sympathetic and lasting interest throughout the preparation of this paper.

Grateful acknowledgement is made to Mrs. Marion Porritt for the typing, Miss Nancy Bowers for the mimeographing and to Miss Mary Melikian for the figures.

The Effect of Shear Stresses on the Carrying Capacity of I-Beams[1]

by

Carl-Fredrik A. Leth[2]

Abstract.

This paper considers the bending of a cantilever I-beam of a ductile metal, such as mild steel, that is loaded by a transverse force at the free end. Taking the length of the beam into account the load carrying capacity can be expressed in terms of the moment at the built-in end that is in equilibrium with the maximum transverse force at which collapse of the beam is imminent, owing to the development of regions of plastic flow. The influence of the length of the beam upon this limit moment is studied in the paper.

As the simplest approximation of the limit moment the fully plastic moment can be taken. From experimental evidence it is known that sufficiently long beams can support a force that is in equilibrium with the fully plastic moment. But it is also observed that for beams that have both a short length and an I-shaped cross-section, the limit moment may be considerably less than the fully plastic moment. The aim of the paper is to obtain theoretical estimates of the maximum moment that these I-beams can develop at the built-in end, assuming that the material exhibits ideal plasticity.

1. The results presented in this paper were obtained in the course of research sponsored by the Office of Naval Research under Contract N7onr-35801 with Brown University.

2. Research Assistant, Graduate Division of Applied Mathematics, Brown University, Providence 12, R. I.

At present a complete three-dimensional solution of the problem seems to be out of the question. Even for a two-dimensional model of the problem it would be very difficult to obtain a complete elastic-plastic solution. The limit analysis theorems of Drucker, Prager and Greenberg are therefore applied. These furnish upper and lower bounds for the limit moment. Two approximate lower bounds are obtained by constructing two different admissible stress fields for a two-dimensional model of the problem. Only the second bound gives estimates of the limit moment for short beams, but both bounds are applicable to long beams. For short beams an upper bound is obtained from a kinematically admissible velocity field, using the appropriate limit analysis theorem.

The first stress field is based on a natural extension of the conventional elastic theory of the bending of beams, modifying this in such a way that at loads above the load at which plastic flow first occurs the yield condition is not violated anywhere. The second stress field is artificial in the sense that it is unrelated to the stress distribution of an elastic beam. Nevertheless, it furnishes in a much shorter way than the first a lower bound for the limit moment, valid for both short and long beams.

Both stress fields yield values of the limit moment which tend towards the fully plastic moment for long beams as the ratio of the beam length to depth is increased. For short beams the second stress field gives a value of the limit moment which differs considerably from the fully plastic moment. For this

reason a velocity field is constructed so that an upper bound is obtained for short beams. This velocity field is based on the failure of the short I-beam primarily because of shear in the web. It is shown by examples that the upper and lower bounds are very close for short beams.

The theoretical results obtained in this paper are compared with the reported experimental data that are concerned with the influence of shear stresses. The experiments give a reasonable confirmation of the theoretical results both for the value of the limit moment and for the computed critical length of the beam below which the carrying capacity rapidly decreases.

A. Introduction.

The problem of the elastic-plastic bending of beams is so complex that at present no rigorous complete solutions have been found. In this paper is presented an approximate treatment of a cantilever I-beam which carries a transverse force parallel to the web at the "free" end, Fig. 1. The purpose is to study the effects of the shear stresses on the carrying capacity of the beam. These may gain importance because of the difference in width of the flange and the web.

In the elastic analysis of the general problem of a beam under end loading an exact solution can be obtained by the seim-inverse method of Saint-Venant. For commonly used beam sections, however, this solution is too complicated to be used in normal engineering practice. Instead an approximate solution is used that is based upon an assumption, introduced by J. Bernoulli, concerning the deformation of the beam. The deflection

of the beam is assumed to take place in such a way that points which initially lie in a plane normal to the center-line after the deformation also form a plane that is normal to the deflected center-line. This condition together with the equilibrium equations and Hooke's law yields results that do not fulfill the compatibility equations. Furthermore if the cross-section is not rectangular the condition of a stress-free cylindrical surface of the beam is violated. These inconsistencies are generally of minor importance, however, as many experiments have shown.

In considering the bending of the beam of Fig. 1 beyond the elastic limit, we have formulated a problem that is of fundamental importance in the theory of limit analysis of structures. It is not appropriate in this paper to discuss the procedures of limit analysis. Such discussions can be found e.g. in the book by Van den Broek [1]* and the papers by Baker [2] and Symonds and Neal [3]. It is sufficient to state that limit analysis of beams and frames is an analysis of failure of these structures associated with the formation of "plastic hinges" in the members of the structure. Plastic hinge sections are defined as those across which rotations of arbitrary magnitudes can occur while a constant bending moment, called the limit moment, M_o, is transmitted. In this paper we discuss the computation of the hinge moment at the base of a cantilever I-beam, since this can be regarded as the basic structural element

* Numbers in square brackets refer to the Bibliography at the end of the paper.

in any continuous beam or rigid frame. We shall compare the limit moment for such a cantilever with the approximation to the limit moment that is commonly used in the applications of limit analysis, namely the "fully plastic moment", M_p. This latter moment is now considered in detail.

Consider first a beam subjected to pure bending. Let the beam have two planes of symmetry and let the moment act in one of them, Fig. 2. Assume the material to follow the perfectly elastic-plastic stress-strain law, i.e., the stress-strain diagram in simple tension of Fig. 3. Moreover let it be assumed that each fiber is in a state of simple tension or compression, so that σ_x is the only non-vanishing stress. The condition that cross-sections remain plane in the elastic part of the beam then yields the distribution of stress over the cross-section that is depicted in Fig. 4. In Fig. 4a the outmost fiber has not reached the yield stress, but in 4b the moment has increased so that the outer part of the cross-section becomes plastic, while the inner part remains in the elastic state. In Fig. 4c the curvature of the beam has taken such a large value that the elastic core in the center can be neglected and the plastic regions are considered to cover the entire cross-section. The bending moment corresponding to this last state is called the fully plastic moment.

In general for a beam having two planes of symmetry, in one of which the load is applied, the fully plastic moment is given by

$$M_p = YZ_p$$

where Z_p is twice the moment of the cross-section area on one side of the middle surface, with respect to the transverse axis of symmetry. In the special case of an I-beam, the fully plastic moment can be considered to consist of two parts, namely the contributions from the flanges and from the web. We then have

$$M_p = M_{pf} + M_{pw}$$

where $M_{pf} = b_1(a^2 - c^2)Y$ and $M_{pw} = bc^2Y$ if the web and flange are assumed to be rectangles, Fig. 5.

Note that the stress distributions of Fig. 4 are not an exact solution even for a rectangular beam in pure bending, as was pointed out by Hill [4]; these stresses are not consistent with continuity of displacements at the elastic-plastic boundary.

In the more general problem of the bending of the beam in the presence of shear forces, the moment varies along the beam, and it is necessary to remove the previous assumption that τ_{xz} is zero. It is shown in the book of Prager and Hodge [5], see also Hodge [6], that τ_{xz} must vanish in the plastic region that spreads in from the outer fibers. Hence the distribution of the longitudinal stress, depicted in Fig. 4, remains unchanged if the other assumptions of the analysis for simple bending are retained. The depth of the plastic region then varies according to the distribution of the moment along the beam. Figure 6 shows the plastic region in the cantilever beam loaded with a shear force at the free end. As the elastic region must carry the total shear force, the shear stresses increase in magnitude towards the built-in end at the center of the beam. Failure by

collapse occurs when the limit moment in the presence of shear is reached at the built-in sections; deflections would then continue under constant load, if geometry changes are neglected, with rotations of arbitrary amounts at the plastic hinge at the built-in end. In most applications of limit analysis the component beams are assumed to be sufficiently long with respect to their depth so that the shear stresses can be neglected in computing the limit moment. Thus the fully plastic moment is taken in these cases as a good approximation of the actual limit moment.

An early paper dealing with the shear stresses at the section of failure of the beam was written by Stüssi [7]. He considers a beam under the influence of a moment and a shear force. Assuming that the longitudinal stress follows a general stress-strain law in simple tension for mild steel and considering plane cross-sections to remain plane over the entire cross-section, the distribution of shear stress is obtained with the help of the equilibrium equation. The fact that the value of the longitudinal stress at yield is affected by the presence of these shear stresses is neglected. The shear stress at the center of the critical cross-section at a specified stage of the loading is considered to form the condition for the failure of beam.

A recent investigation of the shear stresses at the most highly stressed section has been presented by Horne [8]. A rectangular or an I-shaped cross-section under the assumption of plane stress and the Tresca yield condition is treated. At

failure two different plastic regions appear. One of these contains the outer fibers of the beam at the built-in end where longitudinal stresses are large; the other plastic region develops at the center of the beam where shear stresses predominate. The assumption that plane cross-sections remain plane during the deformation is adopted in the elastic region. In the plastic regions account is taken of the equilibrium and yield conditions, but not of strains. It is not possible in this solution to satisfy all the matching conditions of the stresses at the plastic-elastic boundaries. For the case of I-beams the possibility of a violation of the yield condition at the flange-web junction is not investigated.

A different viewpoint is presented in a paper by Onat and Shield [9]. The same problem as in Fig. 1 is treated for a rectangular cross-section with the assumptions of plastic-rigid material and plane strain conditions. The exact solution (fulfilling both stress- and flow-conditions) for the region near the built-in end is obtained.

In the experimental studies of the bending of beams beyond the elastic limit, there are many results showing that for long beams the fully plastic moment provides a good approximation to the limit moment. A survey of these studies has been presented by Roderick and Phillips [10]. On the other hand, relatively few experiments have been made whose aim was to study the behavior of the beam when shear effects are important. Apparently the only extensive tests of this nature are those made by Baker and Roderick [11], Hendry [12], and Johnston,

Yang and Beedle [13]. The comparison of the results of this paper with these experiments is postponed until after the analysis has been described.

B. General concepts.

The analysis in this paper is based upon the two limit analysis theorems of Drucker, Prager and Greenberg [14]. The main part of the paper is concerned with the first of these theorems, and we begin by defining the terms and concepts that are used in it.

A yield function Φ is a positive definite function of the stress components only, such that plastic flow can occur when $\Phi = 1$. In a stress-free state we have $\Phi = 0$ and the elastic range consists of $0 < \Phi < 1$. We then define a safe state of stress as a state for which $\Phi < 1$ throughout the structure. On the other hand collapse is defined as the state for which plastic flow would occur under constant load if the accompanying changes in the geometry of the structure were disregarded. Moreover we call a stress system statically admissible when it satisfies the equilibrium equations and is consistent with the surface tractions on the boundary of the body. The first limit analysis theorem then states that if a safe statically admissible state of stress can be found at each stage of loading, collapse will not occur under the given loading schedule. Thus a load at which a safe statically admissible stress field can be constructed is a lower bound for the collapse load of a structure.

In the main part of this paper we apply the theorem stated above to the problem of estimating a lower bound for the

maximum end force that can be applied to a cantilever beam, Fig. 1. As discussed later in this section we find it necessary to make certain approximations in the construction of safe statically admissible stress fields for this problem. Since the conditions of the theorem are not satisfied exactly, the maximum loads obtained in our analysis cannot be regarded as true lower bounds of the collapse load of the problem. However, it is believed that the nature of the approximations is such that the results will be of practical usefulness, and will serve as a guide to further experiments.

As it is part of our purpose to study plastic regions in the beam we consider stress systems that fulfill the yield condition $\Phi \leq 1$, the equilibrium equations, and agree with the specified surface tractions. We then know that the corresponding load either is the true collapse load or is smaller than this load. This is true because of the fact that any smaller load will be in equilibrium with a safe statically admissible stress-system and therefore cannot be a collapse load. Note that, when using this theorem, we focus our attention entirely on the stresses. This was done also by Horne [8], who dealt primarily with conditions on the stresses. The lower bound theorem provides a basic justification for this point of view.

We shall here use the yield function that was proposed by von Mises. It has the form (see [5])

$$\Phi = \frac{1}{Y^2}\left[\sigma_x^2 + \sigma_y^2 + \sigma_z^2 - \sigma_x\sigma_y - \sigma_y\sigma_z - \sigma_z\sigma_x + 3\tau_{xy}^2 + 3\tau_{yz}^2 + 3\tau_{zx}^2\right].$$

Although we have eliminated above all considerations of compatibility of strains the problem is still so complicated that further simplifications must be made. Following the method of the approximate elastic solution, mentioned in the Introduction, this analysis is made two-dimensional in the x,z plane, so that σ_x, τ_{xz} and σ_z are the only non-vanishing stresses. Moreover we assume the stresses to be independent of the y-coordinate. This implies that the condition of no surface traction on the inner sides of the flanges must be violated. The same error appears in the approximate elastic solution. This cannot, of course, be taken as a justification of the assumption in the problem of the plastic bending of the beam. Such justification must ultimately be found in a more complete theory or by experiments.

Two different stress fields are constructed in the following. In the first analysis (Section C) it is desirable to make a further approximation. This consists of assuming the σ_z stress to vanish, and it turns out that one of the two equilibrium equations cannot generally be satisfied in this case. In the second analysis (Section D) the same assumption is made, but for this stress field it is found that a vanishing σ_z does satisfy both equilibrium equations. Hence no approximation in this regard is involved in the second type of stress field. As this second analysis gives quite satisfactory values of the estimates of the limit moment no attempt is made to consider the effects of the σ_z stress in the first analysis.

The first analysis is built up as a continuation of the conventional elastic theory of the bending of beams. In this theory it is known that the most highly stressed points of long beams are located in the outer fibers at the built-in section. Hence we assume that plastic regions start at these points and then spread in through the flange into the web, Fig. 6. At some stage a new plastic region will form starting from the center point of the web at the built-in section. In this first analysis we estimate the limit load by the load that corresponds to the stage when the stresses at the center of the beam at the built-in section just start to produce plastic flow. The present estimates of limit loads are conservative on this account. The calculation in the first part of the analysis considers this case where the plastic regions have the shape indicated in Fig. 6. However, when the yield condition is checked in the elastic region, we find that a critical point exists at the flange-web junction for beams of relatively short length. This suggests that a second plastic region will occur in the outer portions of the web, as shown in Fig. 7. The second part of this analysis considers this case. In the third part, beams of still shorter lengths are treated, namely the case when the second plastic region extends into a cross-section of the beam that otherwise would have been entirely elastic. This is shown in Fig. 8.

At the start of the second analysis (Section D) a stress field is constructed which is anticipated by the failure of a very short beam due to shear in the web. It is then found possible to generalize this stress field so that beams of arbitrary

lengths can be treated.

The second type of stress field is both simpler and more general than the first type, and it will probably provide the more useful basis for estimating limit moments in the presence of shear forces. On the other hand the second type of stress field is quite artificial, whereas the first type is a natural extension of the well confirmed simple theory of elastic-plastic bending of beams. In this respect it corresponds to and supplements the analysis of Horne [8].

C. Analysis for the first type of stress field.

For the first type of stress field this analysis is divided into three parts, based in turn on the three configurations of plastic regions shown in Figs. 6 - 8. The analysis will show that there exist for a given cross-section shape three decisive lengths l_o, l_1 and l_2 which determine the appropriate configuration.

1. Beams of length so that $l \geq l_1$ and $l \geq l_o$.

We here consider plastic regions as shown in Fig. 6. They are bounded by the outer sides of the flanges, by the built-in section and the curve u(x). In zone BC of the beam the plastic regions extend into the web, but in zone CF the boundaries of the plastic regions are located in the flange. With the assumption $\sigma_z = 0$, the two remaining stresses in the plastic regions are described by the equilibrium equation and by the yield condition:

$$\frac{\partial \sigma_x}{\partial x} + \frac{\partial \tau_{xz}}{\partial z} = 0 \qquad (1)$$

$$(\sigma_x^2 + 3\tau_{xz}^2)\,\frac{1}{Y^2} = 1. \qquad (2)$$

The yield condition (2) is identically satisfied if we relate the stresses to each other through the function $\alpha(x,z)$ in the following manner.

$$\sigma_x = Y \cos\alpha, \quad \tau_{xz} = \frac{Y}{\sqrt{3}} \sin\alpha.$$

The equilibrium equation becomes

$$\sqrt{3}\,\frac{\partial \alpha}{\partial x} \sin\alpha - \frac{\partial \alpha}{\partial z} \cos\alpha = 0. \qquad (3)$$

The characteristics of this equation are lines along which α is constant. The expression

$$d\alpha = \frac{\partial \alpha}{\partial x}\,dx + \frac{\partial \alpha}{\partial z}\,dz = 0$$

together with equation (3) implies that the characteristics are straight lines with the slope

$$\frac{dz}{dx} = -\frac{1}{\sqrt{3}} \cot\alpha. \qquad (4)$$

On the boundary $z = a$ we have $\sigma_x = Y$, $\tau_{xz} = 0$ or $\alpha(x,a) = 0$. The characteristics are therefore lines parallel to the z-axis and the stresses in the plastic region are given by

$$\sigma_x = Y, \quad \tau_{xz} = 0.$$

In the elastic part of the beam we follow the theory based upon the Bernoulli assumption. This implies a tensile stress linear in z. In the elastic part of zone BC we therefore

have

$$\sigma_x = \frac{z}{u} Y.$$

(From here on we consider only positive z-values. The quantities in the beam are either symmetrical or anti-symmetrical around the middle surface.) The equilibrium equation (1) determines the shear stress. Using the boundary condition $\tau_{xz}(x,u) = 0$ we obtain

$$\tau_{xz} = - \frac{u'}{2} (1 - \frac{z^2}{u^2}) Y$$

where the prime denotes differentiation with respect to x. The boundary u(x) between the plastic and elastic regions in the zone BC is determined by the total moment at any cross-section. It is

$$Px = M_p - \frac{1}{3} \frac{u^2}{c^2} M_{pw}$$

or

$$\frac{u^2}{c^2} = 3 \frac{M_p - Px}{M_{pw}} . \qquad (5)$$

The cross-section C is determined by $u_C = c$ or

$$x_C = \frac{M_p - \frac{1}{3} M_{pw}}{P} . \qquad (6)$$

In the elastic part of zone CF we have

$$\sigma_x = \frac{z}{u} Y$$

and the shear stress in the flange is also given by equation (1)

$$\tau_{xz} = - \frac{u'}{2} (1 - \frac{z^2}{u^2}) Y.$$

To find the shear stress in the web we must consider the difference in the width of the beam at the flange-web junction. We

let the equilibrium condition be satisfied only approximately; namely we assume that the shear stress has the same jump at the flange-web junction as the width of the beam. Hence the boundary condition for the shear stress in the web is

$$\tau_{xz}(x,c) = -\frac{b_1}{b}\frac{u'}{2}\left(1 - \frac{c^2}{u^2}\right) Y.$$

The equilibrium equation (1) then gives the shear stress in the web

$$\tau_{xz} = -\frac{u'}{2}\left[1 - \frac{z^2}{u^2} + \left(\frac{b_1}{b} - 1\right)\left(1 - \frac{c^2}{u^2}\right)\right] Y.$$

As before the plastic-elastic boundary u(x) in zone CF is determined by the total moment at any cross-section. It is

$$Px = \left\{ (a^2 - u^2)b_1 + (u^2 - c^2)\frac{c}{u} b_1 + \frac{(u - c)^2}{u} b_1 \left[c + \frac{2}{3}(u - c)\right] + \frac{2}{3}\frac{c^3}{u} b \right\} Y$$

or

$$\frac{u^3}{c^3} - 3\left[\frac{a^2}{c^2} - \frac{Pxb}{M_{pw}b_1}\right]\frac{u}{c} + 2\left(1 - \frac{b}{b_1}\right) = 0. \qquad (7)$$

The cross-section F is determined by $u_F = a$, i.e.,

$$\frac{a^3}{c^3} - 3\left[\frac{a^2}{c^2} - \frac{Px_Fb}{M_{pw}b_1}\right]\frac{a}{c} + 2\left(1 - \frac{b}{b_1}\right) = 0$$

or

$$x_F = \frac{IY}{aP} \qquad (8)$$

where I is the moment of inertia of the cross-section

$$I = \frac{2}{3}\left[b_1a^3 - (b_1 - b)c^3\right].$$

In the entirely elastic zone FH the tensile stress is given by

$$\sigma_x = \frac{P}{I} xz.$$

The equilibrium equation (1) again determines the shear stress, so that

$$\tau_{xz} = \frac{P(a^2 - z^2)}{2I} \qquad \text{in the flange}$$

$$\tau_{xz} = \frac{P(\frac{M_p}{M_{pw}} c^2 - z^2)}{2I} \qquad \text{in the web.}$$

The validity of the stress-system, obtained above, depends on two conditions. First, it is assumed in Fig. 6 that the plastic regions extend into the web at the built-in section. Secondly, the yield function is assumed not to exceed unity in the elastic region. The first condition implies $u_B \leq c$, i.e.,

$$\ell \geq \frac{M_p - \frac{1}{3} M_{pw}}{P} . \tag{9}$$

For the second condition we form the yield function

$$\Phi = (\sigma_x^2 + 3\tau_{xz}^2) \frac{1}{Y^2}$$

in the different parts of the elastic region. We obtain

$$\Phi_{BC} = \frac{z^2}{u^2} + \frac{27}{16} (\frac{Pc}{M_{pw}})^2 \frac{c^2}{u^2} (1 - \frac{z^2}{u^2})^2$$

$$\Phi_{CF} = \frac{z^2}{u^2} + \frac{27}{16} (\frac{Pc}{M_{pw}})^2 (\frac{(u/c)^2 - (z/c)^2}{[(u/c)^3 - 1]b_1/b + 1})^2 \qquad \text{in the flange}$$

$$\Phi_{CF} = \frac{z^2}{u^2} + \frac{27}{16} (\frac{Pc}{M_{pw}})^2 (\frac{1 - (z/c)^2 + [(u/c)^2 - 1]b_1/b}{[(u/c)^3 - 1]b_1/b + 1})^2 \qquad \text{in the web}$$

$$\Phi_{FH} = \frac{P^2}{I^2Y^2}\left[x^2z^2 + \frac{3}{4}(a^2 - z^2)^2\right] \qquad \text{in the flange}$$

$$\Phi_{FH} = \frac{P^2}{I^2Y^2}\left[x^2z^2 + \frac{3}{4}\left(\frac{M_p}{M_{pw}}\,c^2 - z^2\right)^2\right] \quad \text{in the web.}$$

When we look for possible maxima of Φ we notice that in the zone FH Φ has its maximum value at the section F. Hence we need only to check the zones BC and CF.

In the zone BC it is convenient to consider $z^2/u^2 = \xi$ and $27/16\ (Pc/M_{pw})^2\ c^2/u^2 = \eta$ as the two independent variables. Then

$$\Phi_{BC}(\xi,\eta) = \xi + \eta\,(1 - \xi)^2.$$

A maximum appears on the boundaries $\eta = \eta_{max}$ and $\xi = 1$. At $\xi = 1$ we have $\Phi = 1$, so the critical section is $\eta = \eta_{max}$ corresponding to the smallest possible value of u, i.e., the built-in section. The maximum of Φ at this section appears for $z = 0$. As mentioned in the previous section we take the load P_1 as an estimate of the limit load in this analysis, where P_1 is determined by the yield condition at this critical point. Hence we have

$$\frac{27}{16}\left(\frac{P_1 c}{M_{pw}}\right)^2 \frac{c^2}{u_B^2} = 1.$$

u_B is eliminated by means of equation (5). This gives

$$\frac{P_1 \ell}{M_p} = \frac{8}{9}\frac{\ell^2}{c^2}\frac{M_{pw}}{M_p}\left[\sqrt{1 + \frac{9}{4}\frac{c^2}{\ell^2}\frac{M_p}{M_{pw}}} - 1\right]. \qquad (10)$$

The yield condition remains to be checked in zone CF. We find when looking for extreme values that there are no

stationary points in the flange. On the boundaries of the elastic region in the flange we have on one side the plastic region and on the other side the junction to the web. Because of the jump of the shear stresses at this junction the stresses in the web are more critical. The yield function in the web also has maximum on the boundaries, i.e., z = 0 and z = c. At z = 0 we have

$$\Phi_{CF} = \frac{27}{16} \left(\frac{Pc}{M_{pw}}\right)^2 \left(\frac{[(u/c)^2 - 1]b_1/b + 1}{[(u/c)^3 - 1]b_1/b + 1}\right)^2 .$$

As $u/c \geq 1$ Φ_{CF} has maximum for smallest possible u/c, i.e., u = c. But for this value we know from zone BC that the yield condition is satisfied. Hence we have to check at the flange-web junction. We have at z = c

$$\Phi_{CF} = \frac{c^2}{u^2} + \frac{27}{16} \left(\frac{Pc}{M_{pw}}\right)^2 \left(\frac{[(u/c)^2 - 1]b_1/b}{[(u/c)^3 - 1]b_1/b + 1}\right)^2 .$$

Equating $\Phi_{CF} = 1$ yields the following equation in u/c:

$$\left(\frac{u}{c}\right)^3 - 1 + \frac{b}{b_1} = \frac{3\sqrt{3}}{4} \frac{Pc}{M_{pw}} \frac{u}{c} \sqrt{\frac{u^2}{c^2} - 1} \qquad (11)$$

or

$$\left(\frac{u}{c}\right)^6 - \frac{27}{16} \left(\frac{Pc}{M_{pw}}\right)^2 \left(\frac{u}{c}\right)^4 - 2\left(1 - \frac{b}{b_1}\right)\left(\frac{u}{c}\right)^3$$

$$+ \frac{27}{16} \left(\frac{Pc}{M_{pw}}\right)^2 \left(\frac{u}{c}\right)^2 + \left(1 - \frac{b}{b_1}\right)^2 = 0.$$

The last equation shows that there are two or zero positive roots. We can get an approximate solution by considering the quantity $u/c - 1 = \varepsilon$, which is assumed to be a small number as

compared to unity. The equation becomes

$$\sqrt{\varepsilon}\left[\frac{3\sqrt{3}}{4}\frac{Pc}{M_{pw}}(1+\varepsilon)\sqrt{\varepsilon+2}-\sqrt{\varepsilon}\,(3+3\varepsilon+\varepsilon^2)\right]=\frac{b}{b_1}\,.$$

As $\frac{1}{4}\,3\sqrt{3}\,Pc/M_{pw}$ may be of the same order as $\sqrt{\varepsilon}$, we get in approximate form

$$\sqrt{\varepsilon}\left(\frac{3\sqrt{6}}{4}\frac{Pc}{M_{pw}}-3\sqrt{\varepsilon}\right)=\frac{b}{b_1}$$

or

$$\varepsilon=\frac{1}{3}\left\{\frac{9}{16}\left(\frac{Pc}{M_{pw}}\right)^2-\frac{b}{b_1}\pm\sqrt{\left[\frac{9}{16}\left(\frac{Pc}{M_{pw}}\right)^2-\frac{b}{b_1}\right]^2-\left(\frac{b}{b_1}\right)^2}\right\}. \quad (12)$$

The critical value, when yield just starts at one point, corresponds to vanishing of the radical, i.e.,

$$\frac{Pc}{M_{pw}}=\frac{4}{3}\sqrt{\frac{2b}{b_1}}, \quad (13)$$

located at the section where

$$\varepsilon=\frac{u}{c}-1=\frac{1}{3}\frac{b}{b_1}\,.$$

In the cases of I-sections of particular interest here $b/b_1 \sim 0.1$, so that the assumption that ε is small as compared to unity is satisfied.

We now consider the beam loaded with the force P_1 according to equation (10). Then elimination of P_1 between (10) and (13) gives an approximate value of the length of the beam, ℓ_1, for which the two critical points start to yield simultaneously. We obtain

$$\frac{\ell_1}{c}\doteq\frac{3\sqrt{2}}{8}\sqrt{\frac{b_1}{b}}\left(\frac{M_p}{M_{pw}}-\frac{2b}{b_1}\right). \quad (14)$$

On the other hand eliminating P_1 between the inequality (9), taken as an equation, and equation (10) gives

$$\frac{\ell_o}{c} = \frac{\sqrt{3}}{4}\left(3\,\frac{M_p}{M_{pw}} - 1\right). \qquad (15)$$

Hence we have the following two conditions for the validity of this first part of the analysis:

$$\frac{\ell}{c} \geq \frac{\ell_1}{c} \quad \text{and} \quad \frac{\ell}{c} \geq \frac{\ell_o}{c}\,.$$

It is interesting to compare these two values for standard I-beams. Table 1 shows that for many common sections $\ell_1 > \ell_o$. This shows that the stresses at the flange-web junction play a decisive role even for relatively long beams.

The influence of the shear stresses upon the limit moment is expressed by equation (10). This influence is shown in Fig. 9, where $P_1\ell/M_p$ is plotted as function of $\frac{\ell}{c}\sqrt{M_{pw}/M_p}$.

2. Beams of length so that $\ell_1 \geq \ell \geq \ell_2$ and $\ell \geq \ell_o$.

We now consider beams that have a length shorter than ℓ_1. We retain the previous estimate of the limit load as the force P_1 according to equation (10). The stress field must therefore be modified so that the yield condition $\Phi \leq 1$ is satisfied everywhere. We introduce second plastic regions in the web as shown in Fig. 7. These regions are bounded by the curve v(x) and occupy the zone DE, where we assume, in this part of the analysis, that the cross-sections D and E are located between the cross-sections C and F.

There is no reason to change the previous stresses in the zones BD and EH of the beam. The cross-sections D and E are determined by equation (11) or approximately by equation (12). The condition that the cross-section E will be located to the left of cross-section F is given by $u_E \leq a$. By means of equations (8) and (11) this condition is

$$\frac{\ell}{c} \geq \frac{\ell_2}{c} = \frac{\sqrt{3}}{4} \left[K \frac{M_p}{M_{pw}} - \frac{\sqrt{3}}{K} \right] \tag{15}$$

where

$$K = \frac{2a}{IY} \sqrt{\frac{b_1}{b} M_{pw} M_{pf}}.$$

We also assume, as before, that $u_B \leq c$. The bounds for the length of the beam for which this part of the analysis applies, therefore, are

$$\frac{\ell_1}{c} \geq \frac{\ell}{c} \geq \frac{\ell_2}{c} \quad \text{and} \quad \frac{\ell}{c} \geq \frac{\ell_o}{c} .$$

Now consider zone DE. Both the flange and the web are partly elastic, partly plastic. In the plastic region of the flange we have as before $\sigma_x = Y$, $\tau_{xz} = 0$. In the plastic region of the web we again relate the stresses to each other by $\sigma_x = Y \cos \alpha(x,z)$ and $\tau_{xz} = \frac{Y}{\sqrt{3}} \sin \alpha(x,z)$. If the boundary condition at the flange-web junction were given, we then could determine the stresses along the characteristics. Therefore we consider $\alpha(x,c) = f(x)$ as a given function and express further quantities in terms of it.

In the elastic region of the flange the assumption of linear variation of σ_x and of continuity of σ_x and τ_{xz} across the elastic plastic interface then yields

$$\sigma_x = \frac{(u - z)\cos f + z - c}{u - c} Y.$$

The equilibrium equation (1) together with the boundary condition $\tau_{xz}(x,u) = 0$ gives

$$\tau_{xz} = -\frac{1}{2}\frac{\partial}{\partial x}\left[\frac{(u - z)^2}{u - c}(1 - \cos f)\right]Y.$$

The other boundary condition

$$\tau_{xz}(x,c) = \frac{Yb}{\sqrt{3}\, b_1} \sin f$$

determines the function u(x) to within an arbitrary constant A, as follows:

$$(u - c)(1 - \cos f) = A + \frac{2b}{\sqrt{3}\, b_1}\int_x^{x_D} \sin f \, dx.$$

The boundary condition $u = u_D$ at cross-section D determines A so that

$$u = c + \frac{(u_D - c)(1 - \cos f(x_D))}{1 - \cos f} + \frac{2b\int_x^{x_D} \sin f \, dx}{\sqrt{3}\, b_1(1 - \cos f)}. \quad (16)$$

But u is given also at section E. Hence we must impose one condition on the function f, namely

$$\frac{\sqrt{3}\, b_1}{2b}\left[(u_E - c)(1 - \cos f(x_E)) - (u_D - c)(1 - \cos f(x_D))\right] = \int_{x_E}^{x_D} \sin f \, dx. \quad (17)$$

This equation can also be derived as the equilibrium equation of forces in the x direction on the segment at the flange between D and E.

In the second plastic region in the web the stresses are given along each characteristic. Hence $\sigma_x = Y \cos f(x)$ and

$\tau_{xz} = \frac{Y}{\sqrt{3}} \sin f(x)$ where the value of x refers to the coordinate of the characteristic at the flange-web junction, Fig. 10. As before, the characteristics are straight lines in this case making the angle $\varphi(x)$ to the z-direction. In view of equation (4)

$$-\frac{dx}{dz} = \sqrt{3} \tan f = \tan \varphi. \tag{18}$$

It is found convenient to denote the length of the characteristic by $g(x)\ \sqrt{1 + 2 \sin^2 f(x)}$.

Now consider a "cross-section" of the beam that follows the characteristic in the second plastic region as shown in Fig. 10. Due to the slope of the characteristic the center part of this "cross-section" has a coordinate, denoted by s, that differs from the coordinate x of the outer part of the "cross-section". The coordinates are related by

$$s(x) = x + g(x)\ \sqrt{1 + 2 \sin^2 f(x)}\ \sin \varphi(x)$$

$$= x + \sqrt{3}\ g(x) \sin f(x).$$

The function v is now determined at s by

$$v[s(x)] = c - g(x)\ \sqrt{1 + 2 \sin^2 f(x)}\ \cos \varphi(x)$$

$$= c - g(x) \cos f(x).$$

Hence the assumptions of continuity and of linear variation of σ_x gives

$$\sigma_x[s(x),z] = \frac{z \cos f(x)}{c - g(x) \cos f(x)}\ Y.$$

The equilibrium equation is

$$\frac{\partial \sigma_x}{\partial x}\frac{dx}{ds} + \frac{\partial \tau_{xz}}{\partial z} = 0.$$

This determines τ_{xz} together with the boundary condition

$$\tau_{xz}[s(x), c - g\cos f(x)] = \frac{Y}{\sqrt{3}} \sin f(x).$$

We obtain

$$\tau_{xz} = \frac{1}{2}\left[\frac{2}{\sqrt{3}} \sin f + \left(1 - \frac{z^2}{(c - g\cos f)^2}\right)\frac{g'\cos^2 f - cf'\sin f}{1 + \sqrt{3}\,(g \sin f)'}\right] Y.$$

Now it remains to determine g(x) in terms of f(x). As before we set up the equation of total moment, now taken with respect to the point (s,0). The external moment is given by equation (10) as

$$P_1 s = \frac{8}{9}\frac{\ell s}{c^2} M_{pw}\left(\sqrt{1 + \frac{9}{4}\frac{c^2}{\ell^2}\frac{M_p}{M_{pw}}} - 1\right).$$

The plastic regions of the flanges contribute M_1

$$M_1 = (a^2 - u^2)b_1 Y.$$

The elastic regions of the flanges contribute the moment M_2 which is made up of two parts $M_2^{(1)}$ and $M_2^{(2)}$ arising from the tensile and shear stresses, respectively

$$M_2^{(1)} = \frac{1}{3}(u - c)[2u + c + (u + 2c)\cos f]b_1 Y$$

$$M_2^{(2)} = -\frac{1}{\sqrt{3}} g \sin f[(u - c)^2(1 - \cos f)]' b_1 Y$$

$$M_2 = \left\{ \frac{1}{3}(u - c)[2u + c + (u + 2c)\cos f] - \frac{1}{\sqrt{3}} g \sin f\,[(u - c)^2(1 - \cos f)]' \right\} b_1 Y.$$

The plastic regions of the web contribute M_3 which also consists of two parts, $M_3^{(1)}$ and $M_3^{(2)}$, from the two stresses, σ_x and τ_{xz} respectively.

$$M_3^{(1)} = (2c - g\cos f) g \cos^2 f\, bY$$

$$M_3^{(2)} = 2gc \sin^2 f\, bY$$

$$M_3 = (2gc - g^2 \cos^3 f) bY.$$

Finally the elastic part of the web contributes M_4

$$M_4 = \frac{2}{3}(c - g\cos f)^2 \cos f\, bY.$$

The moment equilibrium equation then becomes

$$P_1 s = M_1 + M_2 + M_3 + M_4.$$

It is quadratic in g(x). We therefore obtain

$$g(x) = A(x) - \sqrt{A^2(x) - B(x)} \qquad (19)$$

where

$$A(x) = \frac{c - \frac{3\sqrt{3}}{2}\frac{P_1 c^2}{M_{pw}} \sin f + [2u + \frac{\sqrt{3}\, b_1}{2b}(u - c)^2 f']\sin^2 f}{\cos^3 f} \qquad (20)$$

$$B(x) = \frac{3c^2 \frac{P_1 x - M_{pf}}{M_{pw}} - 2c^2 \cos f + \frac{b_1}{b}(u - c)(u + 2c)(1 - \cos f)}{\cos^3 f}. \qquad (21)$$

To complete the analysis we must write conditions ensuring continuity of stresses at cross-sections D and E. The following requirements are imposed on the values of f(x) and f'(x) at D and E:

$$f(x_D) = \cos^{-1}\left(\frac{c}{u_D}\right); \qquad f'(x_D) = \frac{u_D' c}{u_D\sqrt{u_D^2 - c^2}}. \tag{22}$$

$$f(x_E) = \cos^{-1}\left(\frac{c}{u_E}\right); \qquad f'(x_E) = \frac{u_E' c}{u_E\sqrt{u_E^2 - c^2}}. \tag{23}$$

The previous condition on f(x), (17), now takes the form

$$\frac{\sqrt{3}\, b_1}{2b}\left[\frac{(u_E - c)^2}{u_E} - \frac{(u_D - c)^2}{u_D}\right] = \int_{x_E}^{x_D} \sin f \, dx. \tag{24}$$

Any function f(x) that fulfills these five boundary conditions, equations (22), (23) and (24), and produces plastic regions of the type assumed in Fig. 7 will define a statically admissible system of stresses within the framework of the assumptions we have made. In the numerical example one such function f(x) is chosen.

3. Beams of length so that $\ell_2 \geq \ell \geq \ell_o$.

The beams treated in this part have such length and cross-section dimensions that the plastic region that started from the outer fiber extends into the web, and so that the second plastic region extends into the zone FH, see Fig. 8. The length of the beam must therefore fulfill

$$\frac{l_2}{c} \geq \frac{l}{c} \geq \frac{l_o}{c} .$$

One further condition should be mentioned namely the requirement that the cross-section G does not fall near the free end of the beam.

The same stress field as before is used in the zones BF and GH. The "cross-section" F is given by $u_F = a$, i.e.,

$$(a - c)(1 - \cos f(x_F)) = \frac{(u_D - c)^2}{u_D} + \frac{2b}{\sqrt{3}\, b_1} \int_{x_F}^{x_D} \sin f \, dx. \quad (25)$$

The cross-section G is determined by the yield condition in the web at $z = c$. It is

$$1 = \frac{P_1^2 c^2}{I^2 Y^2} \left[x_G^2 + \frac{3}{4} c^2 \left(\frac{M_{pf}}{M_{pw}}\right)^2 \right]$$

so

$$\frac{x_G}{c} = \sqrt{\frac{I^2 Y^2}{P_1^2 c^4} - \frac{3}{4} \left(\frac{M_{pf}}{M_{pw}}\right)^2}. \quad (26)$$

In the zone FG the flange is entirely elastic, but the web contains the second plastic region, Fig. 8. The stresses in the web are determined as before by the function $f(x)$. The expressions for the stresses in the web remain unchanged, so that in the plastic region of the web along each characteristic, Fig. 11

$$\sigma_x = Y \cos f, \quad \tau_{xz} = \frac{Y}{\sqrt{3}} \sin f$$

and in the elastic region of the web

$$\sigma_x = \frac{z \cos f}{c - g \cos f} Y$$

$$\tau_{xz} = \frac{1}{2}\left\{\frac{2}{\sqrt{3}} \sin f + \left[1 - \frac{z^2}{(c - g \cos f)^2}\right] \frac{g' \cos^2 f - cf' \sin f}{1 + \sqrt{3}\,(g \sin f)'}\right\} Y.$$

In the flange, which is in the elastic state, we let σ_x have linear variation in z and be continuous at the flange-web junction. This gives

$$\sigma_x = \frac{(a - z) \cos f + (z - c)h}{a - c} Y$$

where we denote $\sigma_x(x,a) = Yh(x)$. The function h(x) will be found in terms of f(x). The equilibrium equation (1) together with the boundary condition $\tau_{xz}(x,a) = 0$ determines

$$\tau_{xz} = \frac{a - z}{2(a - c)} [(a + z - 2c)h' - (a - z)f' \sin f]Y.$$

The boundary condition for τ_{xz} at the flange-web junction determines h(x). We have in the flange

$$\tau_{xz}(x,c) = \frac{1}{2}(a - c)(h' - f' \sin f)Y = \frac{bY}{\sqrt{3}\, b_1} \sin f.$$

Hence

$$h = B - \cos f + \frac{2b \int_{x_G}^{x} \sin f \, dx}{\sqrt{3}\, b_1 (a - c)}.$$

The constant B is determined from the condition of continuity of σ_x at the section G. We obtain

$$h = \left(\frac{a}{c} + 1\right) \sqrt{1 - \frac{3}{4}\left(\frac{P_1 c^2 M_{pf}}{IY\, M_{pw}}\right)^2} - \cos f + \frac{2b \int_{x_G}^{x} \sin f \, dx}{\sqrt{3}\, b_1 (a - c)}. \quad (27)$$

But the tensile stress is also given at the section F. This imposes the following condition on f(x):

$$\frac{\sqrt{3}\, b_1}{2b}\left[(a - c)(1 - \cos f(x_F)) - \frac{a^2 - c^2}{c}\sqrt{1 - \frac{3}{4}\left(\frac{P_1 c^2 M_{pf}}{IYM_{pw}}\right)^2}\right] = \int_{x_G}^{x_F} \sin f \, dx. \quad (28)$$

This condition is equivalent to equation (17) applying to zone DE. It also expresses the requirement of the equilibrium of the forces in the x-direction for the segment of the flange between F and G.

We now determine the function g(x) by the overall moment equilibrium equation with respect to the point (s,0), Fig. 11. As before, the external moment is

$$P_1 s = \frac{8}{9}\frac{\ell s}{c^2} M_{pw}\left(\sqrt{1 + \frac{9}{4}\frac{c^2}{\ell^2}\frac{M_p}{M_{pw}}} - 1\right).$$

The contributions to the moment from stresses in the web are as given in the previous section, namely

$$M_3 = (2gc - g^2\cos^3 f)bY$$

$$M_4 = \frac{2}{3}(c - g\cos f)^2 \cos f \, bY.$$

The flange contributes the moment M_2, which consists of two parts, $M_2^{(1)}$ and $M_2^{(2)}$, arising from the tensile stresses and the shear stresses, respectively:

$$M_2^{(1)} = \frac{1}{3}(a - c)[(a + 2c)\cos f + (2a + c)h]b_1 Y$$

$$M_2^{(2)} = \frac{g \sin f}{\sqrt{3}}(a - c)^2 (2h + \cos f)' b_1 Y$$

$$M_2 = \frac{1}{3}(a - c)[(a + 2c)\cos f + (2a + c)h + \sqrt{3}(a - c)g \sin f(2h + \cos f)']b_1 Y.$$

As before the moment equilibrium equation

$$P_1 s = M_2 + M_3 + M_4$$

determines g(x) so that

$$g(x) = A - \sqrt{A^2 - B} \tag{29}$$

where

$$A(x) = \frac{c - \frac{3\sqrt{3}}{2}\frac{P_1 c^2}{M_{pw}} \sin f + [2a + \frac{\sqrt{3}\, b_1}{2b}(a - c)^2 f']\sin f}{\cos^3 f} \tag{30}$$

$$B(x) = \frac{3c^2 \frac{P_1 x}{M_{pw}} - 2c^2 \cos f - \frac{b_1}{b}(a-c)[(a+2c)\cos f+(2a+c)h]}{\cos^3 f}. \tag{31}$$

As before, we must check that the stresses are continuous at the cross-sections F and G. The stresses at section F are given on both sides of the cross-section in terms of f(x). Hence f(x) must be continuous and have a continuous first derivative at x_F. Continuity of the shear stresses at F imposes one more condition, namely $u_F' = 0$. In terms of f(x) this condition takes the form

$$f'(x_F) = -\frac{2}{\sqrt{3}} \frac{a+c}{c^2} \frac{M_{pw}}{M_{pf}} . \qquad (32)$$

At section G the continuity of stresses requires

$$f(x_G) = \sin^{-1} \frac{\sqrt{3}\, P_1 c^2 M_{pf}}{2IY\, M_{pw}}; \qquad f'(x_G) = -\frac{2M_{pw}}{\sqrt{3}c\, M_{pf}}. \qquad (33)$$

Any function f(x) that fulfills the four conditions (28), (32) and (33) and produces stresses of the type assumed in Fig. 8 will, within our assumptions, produce a statically admissible stress field. Note that the position of section F and the value of the function f(x) at F are not determined by the stress conditions. These values may be chosen so that the numerical calculations become as simple as possible. It will be convenient to assign a value for x_F at the very beginning of the computation. Thereafter we construct a stress field in the zone FG by using an f(x) that fulfills the conditions (28), (32) and (33). We then finish the problem in dealing with the zone DF, i.e., we choose an f(x) that fulfills conditions (22), (24) and the values of $f(x_F)$ and $f'(x_F)$ that are obtained from zone FG. The third numerical example in the following section is computed according to this scheme.

4. Numerical examples.

In this section an outline is shown of the computations that determine the shape of the plastic regions for three special cases all applied to an 8 WF 40 beam. The numerical values of the different quantities are given to as many as six significant figures, although of course for practical problems such precision

is meaningless. It is necessary in certain cases to carry this number of significant figures in order to show some of the properties of the analysis.

We have chosen in our examples one of the beams listed in Table 1. This table shows the computed lengths ℓ_o, ℓ_1 and ℓ_2 for some beam sections which have been subjected to laboratory tests [11], [12], [13], and for a few other common beam sections. From these beams the 8 WF 40 section has been chosen for detailed discussion because it has a large value of the ratios M_p/M_{pw} and b_1/b. The cross-section dimensions are given in Table 1. We compute three examples, choosing the length of the beam so that one example is provided for each part of the analysis.

In the first example we consider the shortest possible 8 WF 40 beam in which the second plastic region does not appear. Table 1 gives $\ell_1/c = 21.1$, and we therefore take $\ell/c = 21.1$ for the first example. The estimate for the limit load in this case is given by equation (10) as $P_1\ell/M_p = 0.9895$. The beam contains the zones BC, CF and FH where $x_C/c = 20.48$, (Eq. 6), and $x_F/c = 19.02$, (Eq. 8). The elastic-plastic interface is computed in the zones BC and CF according to equations (5) and (7). The results are shown in Table 2 and in Fig. 12.

In the second example we choose the length ℓ/c so that $\ell_1/c \leq \ell/c \leq \ell_2/c$. We take $\ell/c = 12.5356$. (The actual choice was to make $u_B/c = 0.85$ exactly.) The estimate for the limit load is given by equation (10) as $P_1\ell/M_p = 0.9715$. The beam is divided into the zones BC, CD, DE, EF and FH according to Fig. 7.

The elastic-plastic interface in zone BC is given by equation (5). The results are shown in Table 3. Equation (6) gives $x_C/c = 12.3942$. The cross-sections x_D/c and x_E/c are determined from u_D/c and u_E/c in the following way. Equation (12) determines approximately

$$u_D/c - 1 \doteq 0.00176; \quad u_E/c - 1 \doteq 0.129.$$

Using equation (11) we obtain the more accurate values

$$u_D/c - 1 = 0.00175; \quad u_E/c - 1 = 0.14256.$$

Equation (7) then gives

$$x_D/c = 12.3921; \qquad x_E/c = 11.6367.$$

Cross-section F is determined by equation (8) as

$$x_F/c = 11.5074.$$

The zones CD and EF become so narrow that the boundary values of u/c are sufficient to determine the elastic-plastic interface in these zones. We therefore now focus our attention on zone DE.

In order to construct a solution in zone DE we need to determine the function f(x). This is restricted only by the boundary conditions, which are

$$f(12.3921c) = 0.05917; \quad f'(12.3921c) = - 14.881/c \qquad (22a)$$

$$f(11.6367c) = 0.50488; \quad f'(11.6367c) = - 0.17083/c \qquad (23a)$$

and

$$\int_{11.6367c}^{12.3921c} \sin f \, dx = 0.34083c. \qquad (24a)$$

We must therefore choose a certain form of the function f(x), this choice containing five arbitrary constants so that the above conditions can be satisfied. Note that even if the above conditions are satisfied the choice of f(x) may not be satisfactory due to the fact that the results may not agree with the general type of solution assumed in Fig. 7. E.g., the function v(x) may become parallel at a point with the z-axis or it may become larger than c at some point. Both cases must be avoided. For the choice of f(x) in this case we notice that $f'(x_D)$ is numerically large. This can be taken account of conveniently by choosing the f(x) basically as a parabola with the axis parallel to the x-axis and the vertex near x_D. This suggests the introduction of the new variable y and also of the square root as follows:

$$y = 12.3921 + k - \frac{x}{c}$$

and

$$f(y) = A + B\sqrt{y} + Cy + Dy^2.$$

The five constants k, A, B, C and D are to be determined. The conditions become now

$$f(k) = 0.05917; \qquad f'(k) = 14.881$$

$$f(k + 0.7554) = 0.50488; \qquad f'(k + 0.7554) = 0.17083$$

and

$$\int_{k}^{k+0.7554} \sin f \, dy = 0.34083.$$

Prime denotes differentiation with respect to y. These conditions give

$$k = 0.0054; \quad A = -0.1180; \quad B = 2.6358;$$

$$C = -3.0663; \quad D = 1.1344.$$

The function f is shown in Fig. 13. Equations (16), (18) and (19) determine u, φ and g; see Table 4. The plastic regions are shown in Fig. 14.

As the third example consider the shortest possible length for which the previous analysis applies, i.e., $\ell/c = \ell_o/c = 10.53492$. Very similar considerations apply in this case as compared to the foregoing example. The presentation is therefore shortened. We have the zones CD, DF, FG and GH as in Fig. 8. In this case equation (10) gives $P_1\ell/M_p = 0.9605$. Equation (12) gives $u_D/c - 1 \doteq 0.00119$ and from equation (11) $u_D/c - 1 = 0.001185$. Equations (7) and (26) give $x_D/c = 10.53385$ and $x_G/c = 9.29002$. Conditions (22), (32) and (33) are:

$$f(10.53385c) = 0.04865; \quad f'(10.53385c) = -22.011/c \qquad (22b)$$

$$f'(x_F) = -0.33448/c \qquad (32b)$$

$$f(9.29002c) = 0.60659; \quad f'(9.29002c) = -0.15514/c. \qquad (33b)$$

Conditions (24) and (28) give

$$\int_{9.29002c}^{10.53385c} \sin f \, dx = 0.68354 \qquad (24b) + (28b)$$

$$\int_{9.29002c}^{x_F} \sin f \, dx = 2.9898 \, [\cos f(x_F) - 0.77136]. \qquad (28b)$$

In this example the cross-section F is arbitrarily chosen. We take $x_F = 9.5$.

In zone FG we let

$$f = 0.60659 - 0.15514y + Ay^2 + By^3$$

where

$$y = x/c - 9.29002.$$

The conditions (33b) are satisfied while A and B are determined by (28b) and (32b). The constants become A = 4.1964 and B = - 14.679. The equations (18), (27) and (29) determine φ, h and g in zone FG, see Table 5.

In zone DF we have the following conditions on f(x)

$$f(10.53385c) = 0.04865; \quad f'(10.53385c) = - 22.011/c$$

$$f(9.5c) = 0.62314; \quad f'(9.5c) = - 0.33448/c$$

and

$$\int_{9.5c}^{10.53385c} \sin f \, dx = 0.56189c.$$

Now choose

$$f = A + B\sqrt{y} + Cy + Dy^6$$

where

$$y = 10.53385 + k - x/c.$$

The above five conditions determine k = 0.00171, A = - 0.02903, B = 1.93656, C = - 1.40448 and D = 0.11020. Equations (16), (18) and (19) determine u, φ and g in zone DF, see Table 6. The function f and the plastic regions for this third example are shown in Figs. 15 and 16.

D. A second example of an approximate statically admissible stress field.

The results of the previous analysis in this paper show that for beams that have a length ratio greater than ℓ_o/c the reduction of the limit moment is at most of order 10%. Examples of these reductions are given in Table 1 in the column that shows the value of $P_1\ell/M_p$ for beams having the length ratio ℓ_o/c. The cases where shear stresses become important therefore are expected to occur for beams that have length shorter than ℓ_o. A considerable reduction in the maximum end load of a built-in I-beam may take place when the beam becomes so short that the shear capacity of the web is not sufficient to balance the longitudinal force in the flanges. A failure, as depicted in Fig. 17, may then happen. As cross-sections no longer remain plane and normal to the center-line we can assume that the web carries a small amount of the longitudinal stresses so that in the web the shear stresses nearly reach their yield-value. We shall now construct a statically admissible stress field for this case -- starting with the same assumptions as before -- where this stress field is based on the failure of the web in

pure shear. As depicted in Fig. 18 let the stress field be composed as follows:

$$\sigma_x = 0; \qquad \tau_{xz} = \frac{Y}{\sqrt{3}} \qquad \text{in the web}$$

$$\sigma_x = \frac{bxY}{\sqrt{3}\, b_1(a - c)}; \quad \tau_{xz} = \frac{b(a - z)Y}{\sqrt{3}\, b_1(a - c)} \qquad \text{in the flange.}$$

The equilibrium condition (1) is satisfied everywhere and the yield condition (2) is obviously satisfied in the web. At the flange-web junction the shear stresses are in equilibrium in the same sense as before, and the longitudinal stresses are discontinuous. Such a discontinuity is permissible in the construction of a statically admissible stress field, see [14]. This stress field is valid when the yield condition (2) is not violated in the flanges. The yield condition in the flange takes the form

$$\left[\frac{bx}{\sqrt{3}\, b_1(a - c)}\right]^2 + 3\left[\frac{b(a - z)}{\sqrt{3}\, b_1(a - c)}\right]^2 \leq 1.$$

The left-hand side has its maximum value at $x = \ell$ and $z = c$. The yield condition will therefore be satisfied for beams having a length $\ell \leq \ell_3$ where ℓ_3 is obtained from the following equation:

$$\left[\frac{b\ell_3}{\sqrt{3}\, b_1(a - c)}\right]^2 + 3\left[\frac{b}{\sqrt{3}\, b_1}\right]^2 = 1$$

or

$$\ell_3/c = \sqrt{3}\,(a/c - 1)\sqrt{(b_1/b)^2 - 1}. \qquad (34)$$

This length is computed and shown in Table 1. The estimate of the maximum total shear force, P_2, becomes in this case

$$P_2 = 2bc \frac{Y}{\sqrt{3}} + (a - c)b \frac{Y}{\sqrt{3}} = \frac{1}{\sqrt{3}} (a + c)bY.$$

Therefore

$$\frac{P_2 \ell}{M_p} = \frac{1}{\sqrt{3}} (a/c + 1) \ell/c \frac{M_{pw}}{M_p}. \qquad (35)$$

The above stress field suggests a more general field as depicted in Fig. 19. We let

$\sigma_x = k_1 \frac{x}{c} Y$; $\tau_{xz} = k_1 \frac{a - z}{c} Y$ in the flange

$\sigma_x = k_2 \frac{x}{c} Y$; $\tau_{xz} = k_2 \frac{c - z}{c} Y + k_1 \frac{b_1}{b} (\frac{a}{c} - 1)Y$ in the web.

We assume that the two constants k_1 and k_2 are non-negative. The equilibrium condition (1) is satisfied everywhere in the same sense as before. The yield condition must be checked in the flange and the web. We let k_1 and k_2 be so determined that the yield condition is simultaneously satisfied at the most critical points both in the flange and in the web. In the flange this point is $x = \ell$ and $z = c$. The following equation therefore determines k_1:

$$(k_1 \ell/c)^2 + 3 [k_1(a/c - 1)]^2 = 1$$

$$k_1 = \frac{1}{\sqrt{(\ell/c)^2 + 3(a/c - 1)^2}}.$$

In the web the critical point is $x = \ell$ and $z = 0$. We therefore choose k_2 so that

$$(k_2 \ell/c)^2 + 3[k_2 + k_1 b_1/b(a/c - 1)]^2 = 1$$

$$\frac{k_2}{k_1} = \sqrt{A^2 + B} - A$$

where

$$A = 3\, b_1/b\, \frac{a/c - 1}{(\ell/c)^2 + 3}$$

$$B = \frac{(\ell/c)^2 - 3(a/c - 1)^2[(b_1/b)^2 - 1]}{(\ell/c)^2 + 3}.$$

The condition $k_1 \geq 0$ is satisfied but the condition $k_2 \geq 0$ shows that $B \geq 0$, and this restricts the length of the beam. This restriction is

$$\ell/c \geq \sqrt{3}\,(a/c - 1)\sqrt{(b_1/b)^2 - 1} = \ell_3/c. \qquad (36)$$

This stress field together with the previous one therefore applies to any length of the beam. The total shear force now becomes

$$P_2 = k_1(a/c - 1)(a - c)b_1Y + 2k_1(a/c - 1)b_1cY + k_2bcY.$$

Therefore

$$\frac{P_2\ell}{M_p} = \frac{M_{pw}}{M_p}\frac{\ell}{c}\left\{k_1[(a/c)^2 - 1)]\,b_1/b + k_2\right\}. \qquad (37)$$

Within our assumptions equations (35) and (37) provide a lower bound for the limit load. The curve of $P_2\ell/M_p$ versus ℓ/c has been computed for the 8 WF 40 section. The result is shown in Table 7 and in Fig. 21.

In this stress field the assumption that σ_z vanishes is strictly valid. This is true because the shear stresses are independent of x so that the equilibrium equation involving σ_z is identically satisfied. The stress fields that we have constructed give a lower bound for the collapse load. In the next

section we shall obtain an upper bound which will be applicable for short beams.

E. A kinematically admissible velocity field for short beams.

We shall now make use of the second limit analysis theorem of Drucker, Prager and Greenberg [14], which states that a load obtained in a definite manner from a kinematically admissible velocity field is an upper bound for the collapse load. A velocity field is defined as kinematically admissible when it satisfies the imposed velocity conditions at the boundary of the body and when the velocities vanish on those parts of the boundary where the surface tractions are not prescribed. In this paper we consider only velocity fields which are continuous and satisfy the condition of incompressibility

$$\frac{\partial u}{\partial x} + \frac{\partial v}{\partial y} + \frac{\partial w}{\partial z} = 0$$

where u, v and w are the velocity components in the x,y and z directions. The upper bound P* of the load is obtained by equating the rate of work produced by the applied forces to the rate of plastic work in the body.

It seems intuitively likely that a reasonable upper bound of the collapse load should be such that the value $P^*\ell/M_p = 1$ is exceeded by only a small amount, if at all. For moderately long I-beams we have only been able to construct velocity fields that give $P^*\ell/M_p$ considerably larger than unity. We therefore confine attention to short beams where a "good" velocity field is easily obtained and restrict ourselves to the

length of the beams so that $P^*\ell/M_p \leq 1$. The velocity field that is chosen is depicted in Fig. 20. It is symmetric with respect to the middle surface OFG. Part ABFG is rigid and fixed. The part BCDE of the flange is rigid and rotates with the angular velocity ω about the fixed point B. In part ABC of the flange let

$$u = w = -\frac{1}{2}\omega(\ell - x - a + z); \quad v = 0.$$

This is a motion parallel to AB, with velocities continuous on AB and BC. In part BEOF of the web let

$$u = v = 0; \quad w = -\omega(\ell - x - a + c).$$

The velocity is continuous on BE and the motion is parallel to BF. As before we use the von Mises yield condition and therefore also the von Mises flow rule. We have constructed a plane velocity field. The rate of plastic work, W_p, for such fields is derived in [5], page 214.

$$W_p = \frac{Y}{\sqrt{3}} \int \dot{\Gamma} dV$$

where dV is the volume element and $\dot{\Gamma}$ is given by

$$\dot{\Gamma} = [(\frac{\partial u}{\partial x} - \frac{\partial w}{\partial z})^2 + (\frac{\partial u}{\partial z} + \frac{\partial w}{\partial x})^2]^{1/2}.$$

We obtain both in ABC and BEOF

$$\dot{\Gamma} = \omega.$$

The rate of plastic work therefore is

$$W_p = \frac{2}{\sqrt{3}} Y\omega[V_{ABC} + V_{BEOF}]$$

$$W_p = \frac{2}{\sqrt{3}} M_{pw}\omega[b_1/b(a/c - 1)^2 + \ell/c - a/c + 1].$$

The rate of external work is W_e

$$W_e = P^*\omega(\ell - a + c).$$

The limit analysis theorem therefore gives the following upper bound for the limit moment

$$\frac{P^*\ell}{M_p} = \frac{2}{\sqrt{3}} \frac{M_{pw}\ell}{M_p c} \left\{ \frac{b_1/b(a/c - 1)^2}{\ell/c - a/c + 1} + 1 \right\} \tag{38}$$

$P^*\ell/M_p$ becomes unity for

$$\ell/c = A + \sqrt{A^2 - B}$$

where

$$A = \frac{1}{4} [\sqrt{3}\, M_p/M_{pw} - 2b_1/b\,(a/c - 1)^2 + 2(a/c - 1)]$$

and

$$B = \frac{\sqrt{3}}{2} M_p/M_{pw}\,(a/c - 1).$$

This upper bound, computed for the 8 WF 40 section, is shown in Table 7 and plotted in Fig. 21 as a function of ℓ/c. It is seen that the curve for the upper bound load P^* lies parallel to and only slightly higher than that for the lower bound load P_2 corresponding to shear failure in the web.

F. <u>On the relations between experiments and theory</u>.

The example of the curve $P_2\ell/M_p$ versus ℓ/c in Fig. 21 clearly shows that the theory predicts a certain length ratio of the beam below which the load carrying capacity of the beam decreases abruptly, because of shear failure of the web. This critical length ratio is ℓ_3/c. In the following comparison we

therefore look first for the appearance of such a critical length ratio in the experiments, and, when observed, we compare the values of the experimental and the theoretical length ratios.

Secondly we want obviously to compare the experimental and theoretical values of the limit moment in each case. The theoretical values are given by equations (35), (37) (which furnish lower bounds) and (38) (which gives an upper bound, valid for short beams). In the following experimental data from three sources are considered. In the paper by Johnston, Yang and Beedle [13] shear failures in the web of I-beams are reported, but details concerning the length ratios and limit moment values are not given. Baker and Roderick [11] made an investigation of the influence of shear on the limit moment of a particular beam section and presented the results in the form of load-deflection curves from which the variation of limit moment with length ratio can be studied. Hendry [12] has discussed tests on a series of beams of different cross-sections and gives the results in a table where the limit moment was defined by deflection considerations. Adopting his definition of limit moment comparsions are made in this section between the experimental results and the theoretical predictions both as to critical length ratio and magnitude of limit moment.

In the eighth Progress Report from Lehigh University [13] two examples of beams are shown where the collapse of the beams was apparently caused by shear failure in the web. The first example is a 4 I 7.7 beam that is simply supported and loaded symmetrically by two concentrated forces. Each end of

the beam can therefore be represented by the cantilever problem discussed in this paper. The length ratio ℓ/c in the test is approximately 2.5. In the theory equation (34) gives $\ell_3/c = 2.5$, as shown in Table 1.

In the second example an 8 WF 40 beam is loaded so that moments numerically equal but opposite in sense act at the ends of the half-beam, whose length ratio was approximately 16. Because of the symmetrical properties of the load each quarter of the span can be represented by the cantilever beam. The effective length ratio therefore is $\ell/c = 8$. For this case we compute $\ell_3/c = 6.0$.

The ratio between the collapse moment and the fully plastic moment is not stated for these two examples. The tests show that shear failure in the web is important for beams having the above cross-sections and the effective length ratio approximately ℓ_3/c.

Simply supported beams acted upon by two concentrated loads, symmetrically spaced, have been investigated and reported by Baker and Roderick [11]. The beam is a British H-section with dimensions $1\frac{1}{4}$" x $1\frac{1}{4}$". The distance between the loads was kept constant and the span was varied. Different effective length ratios of the corresponding cantilever beam problem were therefore obtained, varying from 9.4 (Test No. SR 21) to 2.2 (Test No. SR 11). The value of ℓ_3/c is 6.7. The load-deflection curves are given. For length ratios greater than 3.9 the curves show a well defined "bend" where the slope of the curve rapidly decreases. The load at these "bends" is

taken as the collapse load in Table 8 and Fig. 22. The table and the figure show that in the experiment when the length ratio is smaller than 5.5 the collapse moment decreases rapidly with further decrease in length ratio. In the theory we have $\ell_3/c = 6.7$ below which $P_2\ell/M_p$ decreases rapidly.

In the paper by Hendry [12] the influence of shear forces in simply supported beams of various I-sections is discussed. In these tests a concentrated load acts on the midpoint of the beam. A series of tests is also included in which the influence of shear stresses in the beam of a portal is investigated. The value of M/M_p is tabulated in the paper, where the moment M is obtained from the load at which the deflection of the beam equals 1/50 of the span. These values are shown in Table 9 and Figs. 23 and 24 together with the theoretical values of $P\ell/M_p$. Except for the portals and the beam 3b we see that M/M_p is in the neighborhood of and is greater than $P_2\ell/M_p$. We notice moreover that for length ratios shorter than ℓ_3/c the value M/M_p is considerably less than unity.

The portals B1 - B5 are made up of a 3" x 1" beam and of 1¼" x 1" stanchions. The ratio of the fully plastic moment of the beam to that of the stanchion is approximately 7.3 to 1. The effective length ratio ℓ/c is therefore taken to be $\frac{7.3}{7.3 + 1} (\ell/c)^* = 0.88\ (\ell/c)^*$ where $(\ell/c)^*$ is the length ratio between the load and the end of the beam. The results in Table 9 show that the portals did not develop the moment $P_2\ell/M_p$.

In [12] the large reduction of the limit moment is explained by the influence of the axial stresses in the columns.

In general we see that the theory and experimental tests agree rather well, with very few exceptions. For this comparison between the experiments and the theory we have used the results obtained by the second type of stress field. This is done because the length ratio is in these cases so short that the first type of stress field does not apply.

G. Summary and conclusions.

The two types of stress field in this paper each give an approximate lower bound for the true collapse load of the plastic bending of a cantilever I-beam. The approximations consist in both cases of a two-dimensional formulation of the problem while in the first type of stress field the further assumption is made that the σ_z stress is negligible. The velocity field, which is applied for short beams, gives results which are upper bounds to the true collapse load. The velocity field satisfies all the requirements of the appropriate theorem of limit analysis. The upper and lower bounds differ by small amounts for short beams. For long beams the lower bounds furnished by both types of stress field tend toward the result $P\ell/M_p = 1$.

The ratio $P_2\ell/M_p$, where P_2 is the lower bound on the collapse load defined in Section D, can be used to estimate the limit moment $M_o = P_2\ell$ in the relation to the fully plasitc moment M_p which is appropriate for pure bending (or very long

cantilevers). We note that the curve of $P_2\ell/M_p$ as function of ℓ/c has two distinct parts, as exemplified by the curves of Figs. 21 - 24. For $\ell/c \leq \ell_3/c$ it is a straight line through the origin with the slope $\frac{a/c + 1}{\sqrt{3}\ M_p/M_{pw}}$. For $\ell/c \geq \ell_3/c$ the value of $P_2\ell/M_p$ increases asymptotically to the value $P_2\ell/M_p = 1$. The reduction of the limit moment at the length ratio ℓ_3/c may be as high as 30% for the beams mentioned in Table 1. The curves show that a much larger reduction of the limit moment takes place when the length ratio is less than ℓ_3/c, but for beams having a length ratio greater than ℓ_3/c the fully plastic moment is generally reduced by a relatively small amount. Table 1 also shows that the value of ℓ_3/c in some cases is so short that in the practical problem the effects of the details of the end constraint or of the loading are very important. It is therefore suggested that beams should not be used whose length ratio is smaller than ℓ_3/c or which are so short that the end effects are important. For example, if $\ell/c < 6$ treatment as a "beam" in the conventional sense is hardly appropriate.

The influence of buckling, particularly of the web or the flange, (or both), is disregarded in this paper. This may be important for certain short beams, as indicated in [13], and should be further investigated.

Bibliography

1. "Theory of Limit Design" by J. A. Van den Broek. John Wiley & Sons, Inc., New York, 1948.

2. "A Review of Recent Investigations into the Behaviour of Steel Frames in the Plastic Range" by J. F. Baker. Jour. Instn. Civil Engrs., Vol. 31, 1949, p. 188.

3. "Recent Progress in the Plastic Methods of Structural Analysis" by P. S. Symonds. Jour. Franklin Inst., Vol. 252, 1951, p. 383.

4. "The Mathematical Theory of Plasticity" by R. Hill. Clarendon Press, Oxford, 1950.

5. "Theory of Perfectly Plastic Solids" by W. Prager and P. G. Hodge, Jr. John Wiley & Sons, New York, 1951.

6. "An Introduction to the Mathematical Theory of Perfectly Plastic Solids" by P. G. Hodge, Jr. Tech. Report A11-S2 of Brown University to ONR under Contract N7onr-35801, February, 1950.

7. "Ueber den Verlauf der Schubspannungen in auf Biegung beanspruchten Balken aus Stahl" by F. Stüssi. Schweizerische Bauzeitung, Vol. 98, No. 1, 1931, p. 2.

8. "The Plastic Theory of Bending of Mild Steel Beams with Particular Reference to the Effect of Shear Forces" by M. R. Horne. Proc. Roy. Soc. Vol. 207-A, 1951, p. 216.

9. "The Influence of Shearing Forces on the Plastic Bending of Wide Beams" by E. T. Onat and R. T. Shield. Tech. Report A11-103 of Brown University to ONR under Contract N7onr-35801, December, 1953.

10. "The Carrying Capacity of Simply Supported Mild Steel Beams" by J. W. Roderick and I. H. Phillips, Research Engineering Structures Supplement (Calston Papers, Vol. II) 1949, p. 9.

11. "Investigation into the Behaviour of Welded Rigid Frame Structures. Second Interim Report; Further Tests on Beams and Portals" by J. F. Baker and J. W. Roderick, Transactions Inst. of Welding, Vol. 3, 1940, p. 83.

12. "An Investigation of the Strength of Certain Welded Portal Frames in Relation to the Plastic Method of Design" by A. W. Hendry. The Structural Engineer, Vol. 28, 1950, p. 311.

13. "An Evaluation of Plastic Analysis as Applied to Structural Design" by B. G. Johnston, C. H. Yang and L. S. Beedle. Welding Research Supplement, Vol. 32, 1953, p. 224.

14. "Extended Limit Design Theorems for Continuous Media" by D. C. Drucker, W. Prager and H. J. Greenberg. Quart. Appl. Math. Vol. 9, 1952, p. 389.

Beam	See Ref	a	h	b_1	c	$\frac{M_p}{M_{pw}}$	b_1/b	ℓ_1/c	ℓ_2/c	i_o/c	ℓ_3/c	$P_1 i/M_p$ at i_o/c	$P_2 \ell/M_p$ at i_3/c	$P*\ell/M_p$ at ℓ_3/c
8 WF 40	10	4.125	0.365	8.077	3.567	8.44	22.13	21.1	12.2	10.5	6.0	0.960	0.881	0.892
14 WF 30	10	6.93	0.270	6.78	6.55	4.03	25.12	10.5	8.4	4.8	2.6	0.918	0.711	0.758
14 WF264	--	8.25	1.205	16.03	6.31	10.42	13.30	19.9	$<i_o/c$	13.1	7.1	0.968	0.904	0.929
15I 42.9	--	7.50	0.410	5.50	6.88	3.55	13.41	6.6	5.7	4.2	2.1	0.907	0.714	0.722
8 I 18.4	--	4.00	0.270	4.00	3.56	4.86	14.81	9.6	7.3	5.9	3.1	0.931	0.790	0.800
4 I 7.7	10	2.00	0.190	2.66	1.81	4.04	14.00	7.7	6.3	4.8	2.5	0.918	0.742	0.752
8x4 RSJ	5	4.00	0.280	4.00	3.60	4.33	14.29	8.4	6.7	5.2	2.7	0.923	0.762	0.772
4x3 RSJ	9	2.00	0.240	3.00	1.65	6.80	12.50	12.5	$<i_o/c$	8.4	4.5	0.951	0.846	0.866
3x1½RSJ	9	1.50	0.160	1.50	1.25	5.10	9.38	7.9	$<\ell_o/c$	6.2	3.2	0.935	0.792	0.811
3x1 I	9	1.50	0.160	1.00	1.25	3.73	6.25	4.5	$<\ell_o/c$	4.4	2.1	0.912	0.705	0.727
1¼ x 1 I	9	0.63	0.125	1.00	0.50	5.50	8.00	7.9	$<i_o/c$	6.7	3.4	0.939	0.798	0.823
1¼x1¼ H	8	0.63	0.125	1.25	0.45	10.73	10.00	17.7	$<\ell_o/c$	13.5	6.7	0.969	0.893	0.925

Table 1. Beam dimensions and computed values

x/c	21.1	21.0	20.9	20.8	20.7	20.6	20.5	20.48
u/c	0.515	0.619	0.709	0.788	0.860	0.927	0.989	1.001

x/c	20.4	20.2	20.0	19.8	19.6	19.4	19.2	19.02
u/c	1.027	1.059	1.082	1.100	1.116	1.131	1.145	1.156

Table 2. The function u/c for 8 WF 40 section; $\ell/c = 21.1$

x/c	12.5356	12.5	12.45	12.3942
u/c	0.85	0.8901	0.9436	1.0000

Table 3. The function u/c in zone BC for 8 WF 40 section; $\ell/c = 12.5356$

x/c	y	f	u/c	φ	g/c	$g/c\sqrt{1+2\sin^2 f}$
12.3921	0.0054	0.05917	1.00175	5.9°	0.0000	0.0000
12.3875	0.01	0.11504	1.0036	11.3°	0.0011	0.0011
12.3775	0.02	0.19390	1.0056	18.8°	0.0079	0.0082
12.3675	0.03	0.24759	1.0072	23.6°	0.0166	0.0176
12.3575	0.04	0.28835	1.0087	27.2°	0.0250	0.0270
12.3475	0.05	0.32094	1.0101	29.9°	0.0344	0.0377
12.3275	0.07	0.37032	1.0128	33.9°	0.0497	0.0573
12.2975	0.1	0.42025	1.0169	38.5°	0.0666	0.0769
12.2475	0.15	0.46845	1.0241	41.2°	0.0814	0.0966
12.1975	0.2	0.49291	1.0319	42.9°	0.0852	0.1025
12.0975	0.3	0.50793	1.0500	44.0°	0.0744	0.0903
11.9975	0.4	0.50408	1.0711	43.7°	0.0536	0.0649
11.8975	0.5	0.49631	1.0940	43.2°	0.0317	0.0383
11.7975	0.6	0.49235	1.1163	42.9°	0.0139	0.0167
11.6975	0.7	0.49679	1.1347	43.2°	0.0031	0.0038
11.6367	0.7608	0.50488	1.1426	43.7°	0.0000	0.0000

Table 4. The functions f, u/c, φ and g/c in zone DE for 8 WF 40 section; $\ell/c = 12.5356$

x/c	y	f	h	φ	g/c	$g/c\sqrt{1+2\sin^2 f}$
9.2900	0	0.60659	0.94976	50.2°	0	0
9.3400	0.05	0.60749	0.95982	50.3°	0.0057	0.0073
9.3900	0.1	0.61836	0.97569	51.0°	0.0167	0.0216
9.4400	0.15	0.62820	0.99119	51.5°	0.0268	0.0349
9.4900	0.2	0.62599	0.99972	51.4°	0.0307	0.0399
9.50	0.2100	0.62314	1.00000	51.2°	0.0301	0.0390

Table 5. The functions f, h, φ and g/c in zone FG for 8 WF 40 section; $\ell/c = 10.53492$

ℓ/c	26	24	22	20	18	16	14	12	10.5
$P_1\ell/M_p$	0.993	0.992	0.990	0.988	0.986	0.982	0.977	0.969	0.961
$P_2\ell/M_p$	0.995	0.994	0.993	0.991	0.989	0.986	0.982	0.975	0.968
ℓ/c	10	9	8	7	5.97	5	4	3	2
$P_2\ell/M_p$	0.964	0.955	0.942	0.922	0.881	0.737	0.590	0.442	0.294
$P^*\ell/M_p$	--	--	--	--	0.892	0.760	0.624	0.448	0.353

Table 7. The values of $P_1\ell/M_p$, $P_2\ell/M_p$ and $P^*\ell/M_p$ for 8 WF 40 section

x/c	y	f	u/c	φ	g/c	$g/c\sqrt{1 + 2\sin^2 f}$
10.53385	0.00171	0.04865	1.00118	4.8°	0.0000	0.0000
10.52556	0.01	0.15059	1.00391	14.7°	0.0027	0.0027
10.51556	0.02	0.21675	1.00597	20.9°	0.0086	0.0090
10.50556	0.03	0.26127	1.00761	25.1°	0.0159	0.0169
10.49556	0.04	0.30210	1.00905	28.4°	0.0236	0.0256
10.48556	0.05	0.33378	1.01038	31.0°	0.0316	0.0348
10.46556	0.07	0.38504	1.01283	35.1°	0.0475	0.0538
10.43556	0.10	0.44292	1.01626	39.4°	0.0698	0.0817
10.40556	0.13	0.48664	1.01956	42.5°	0.0892	0.1069
10.37556	0.16	0.52087	1.02282	44.8°	0.1051	0.1284
10.33556	0.20	0.55613	1.02718	47.1°	0.1211	0.1511
10.28556	0.25	0.58816	1.03278	49.1°	0.1341	0.1705
10.23556	0.30	0.61040	1.03865	50.5°	0.1409	0.1814
10.18556	0.35	0.62529	1.04488	51.3°	0.1426	0.1851
10.13556	0.40	0.63443	1.05153	51.9°	0.1400	0.1827
10.03556	0.50	0.63981	1.06640	52.2°	0.1250	0.1636
9.93556	0.60	0.63348	1.08367	51.8°	0.1010	0.1317
9.83556	0.70	0.62103	1.10313	51.1°	0.0704	0.0912
9.73556	0.80	0.60840	1.12431	50.3°	0.0468	0.0602
9.63556	0.90	0.60268	1.14346	50.0°	0.0284	0.0364
9.53556	1.00	0.61325	1.15507	50.6°	0.0257	0.0331
9.50000	1.03556	0.62314	1.15606	51.2°	0.0309	0.0400

Table 6. The functions f, u/c, φ and g/c in zone DF for 8 WF 40 section; $\ell/c = 10.53492$

Test No.	ℓ	ℓ/c	2W	$W\ell/c$	$P_2\ell/M_p$	$P^*\ell/M_p$
SR 21	4.25	9.44	2.05	9.68	0.918	> 1
20	3.75	8.33	2.30	9.58	0.904	> 1
19	3.25	7.22	2.65	9.57	0.881	0.949
22	3.00	6.67	2.85	9.50	0.857	0.891
17	2.75	6.11	3.05	9.32	0.785	0.831
16	2.50	5.56	3.30	9.17	0.715	0.773
15	2.25	5.00	3.15	7.88	0.643	0.715
10	2.00	4.44	3.15	6.99	0.571	0.656
14	1.75	3.89	3.30	6.42	0.500	0.600

Table 8. The tests by Baker and Roderick

Beam No.	Section	ℓ	ℓ/c	$P_2\ell/M_p$	$P^*\ell/M_p$	M/M_p
1a		15	9.1	0.973	> 1	0.95
b	4" x 3" R.S.J.	12	7.3	0.953	> 1	1.00
c	$\ell_3/c = 4.5$	9	5.5	0.909	> 1	1.00
d		6	3.6	0.684	0.719	0.83
e		4.5	2.7	0.511	0.565	0.71
2a		12	9.6	0.979	> 1	1.00
b	3" x 1½"R.S.J.	7.5	6.0	0.941	> 1	0.97
c	$\ell_3/c = 3.2$	5	4.0	0.869	0.995	0.88
d		3	2.4	0.598	0.636	0.59
3a	3" x 1" R.S.J.	9	7.2	0.967	> 1	0.96
b	$\ell_3/c = 2.1$	4	3.2	0.847	> 1	0.73
3c		10	7.0	0.966	> 1	1.00
d	3" x 1" I	7	4.9	0.929	> 1	0.87
e	$\ell_3/c = 2.1$	5.5	3.9	0.889	> 1	0.86
f	Portals	4	2.8	0.814	0.98	0.61
g	B1 - B5	4	2.8	0.814	0.98	0.76
4a		10	20	0.993	> 1	1.00
b	1¼" x 1" I	5	10	0.975	> 1	1.00
c	$\ell_3/c = 3.4$	3	6	0.934	> 1	0.97
d		1.5	3	0.709	0.744	0.76

Table 9. The tests by Hendry

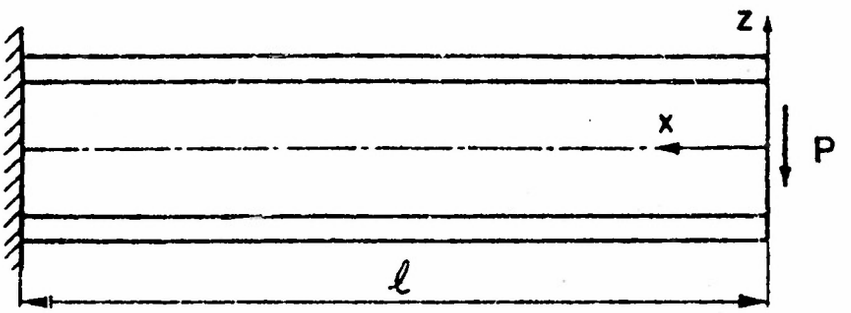

Fig. 1

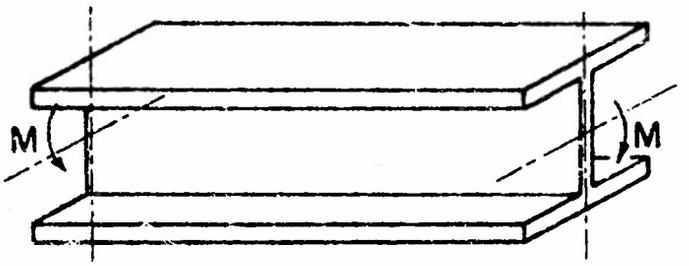

Fig. 2

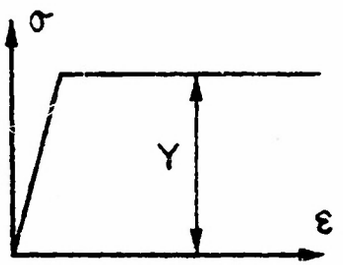

Fig. 3

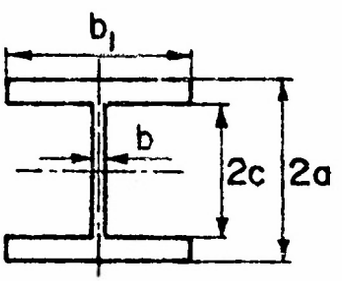

Fig. 5

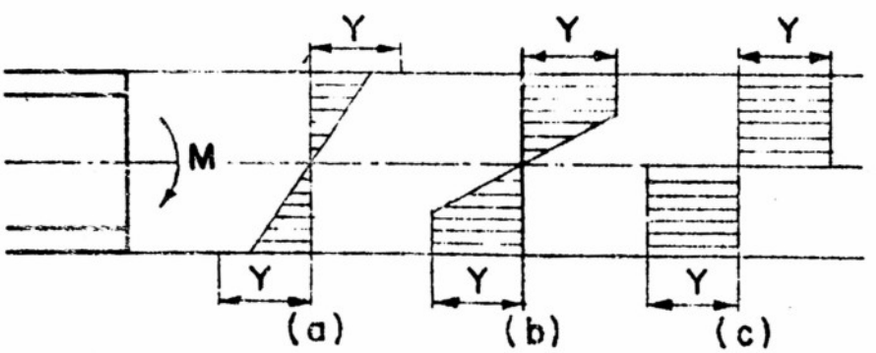

Fig. 4

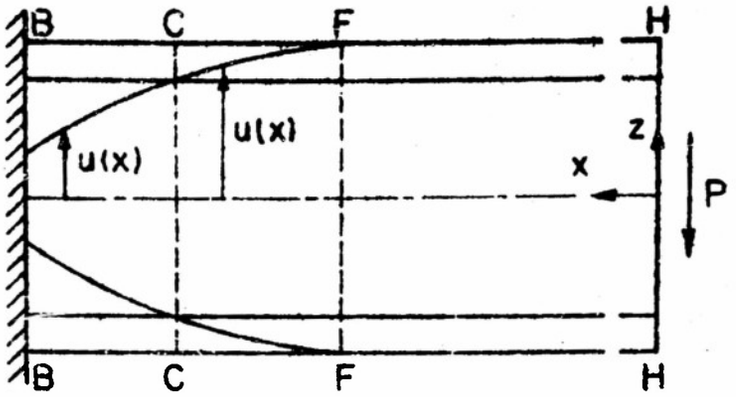

Fig. 6 The shape of the plastic regions for $l \geq l_1$ and $l \geq l_0$

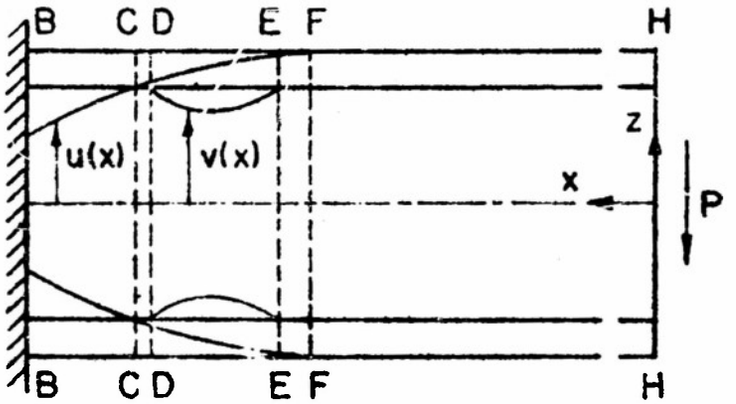

Fig. 7 The shape of the plastic regions for $l_1 \geq l \geq l_2$ and $l \geq l_0$

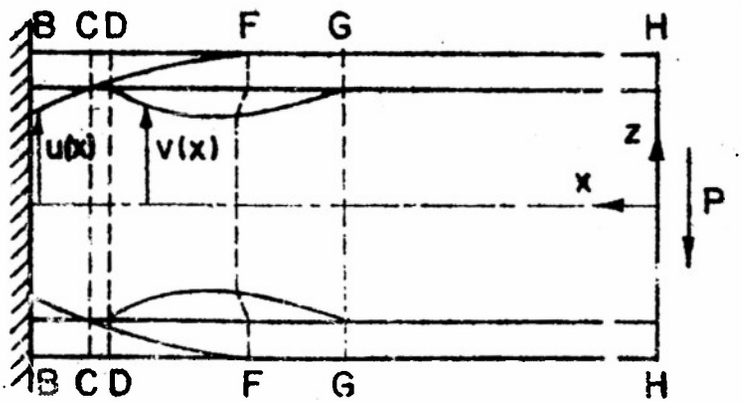

Fig. 8 The shape of the plastic regions for $l_2 \geq l \geq l_0$

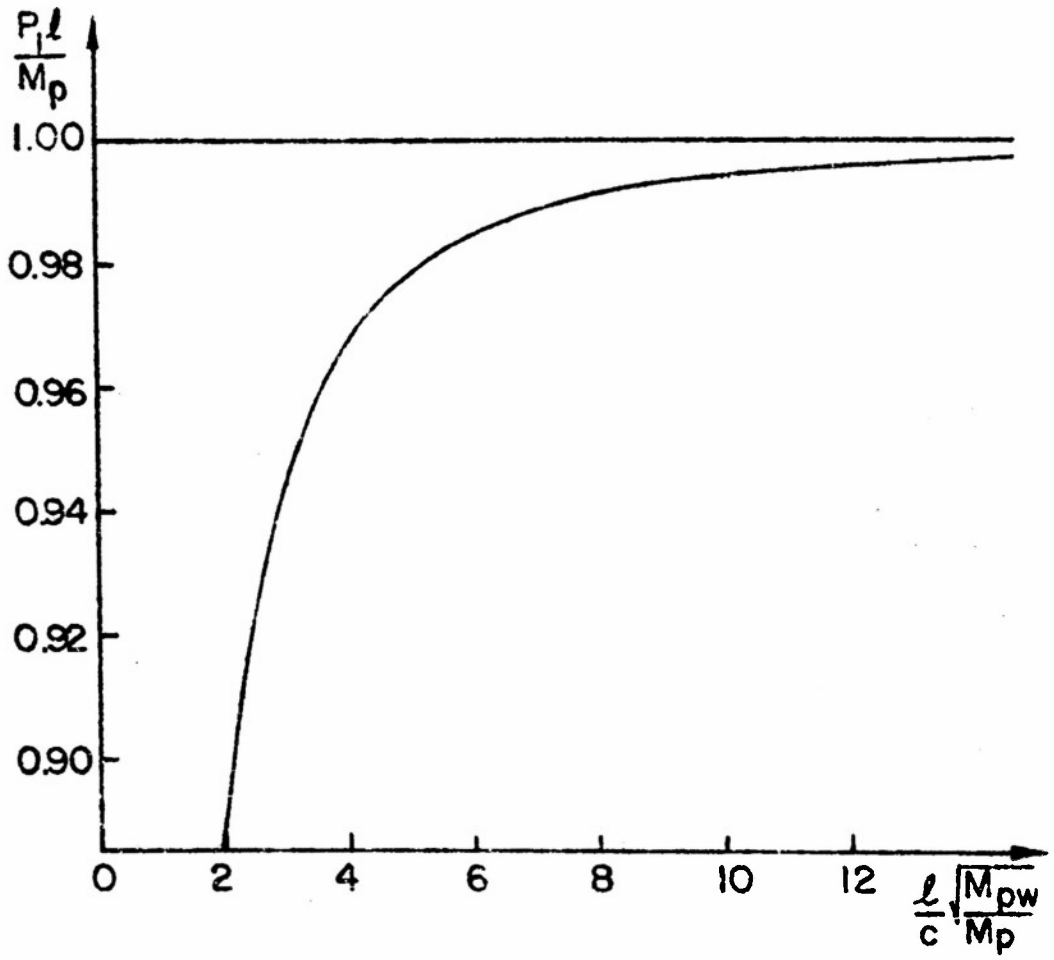

Fig. 9. The ratio $P_1 \ell / M_p$ of the first type of stress field

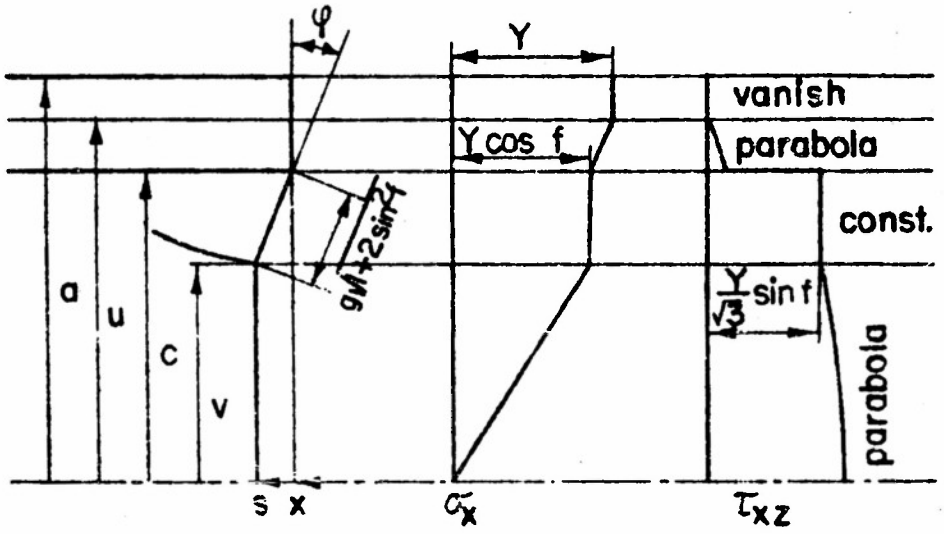

Fig. 10 The stresses at a cross-section in DE

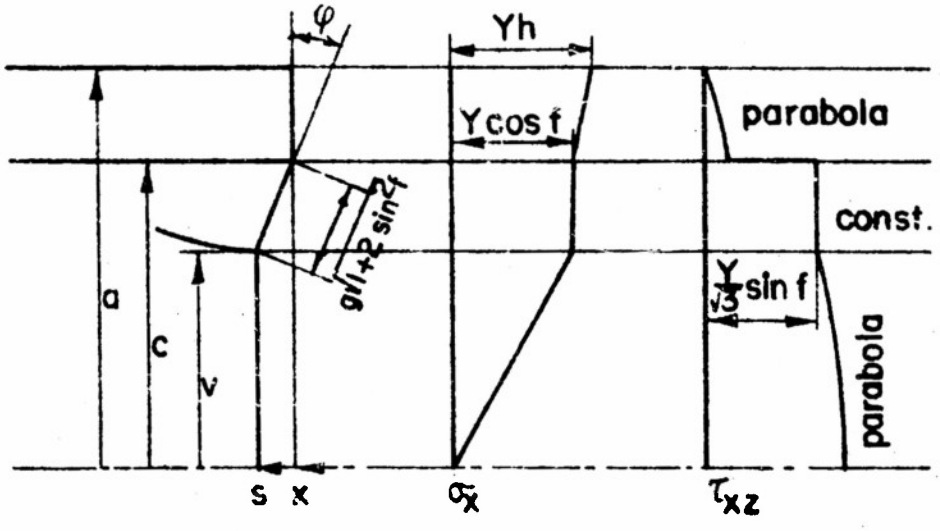

Fig. 11 The stresses at a cross-section in FG

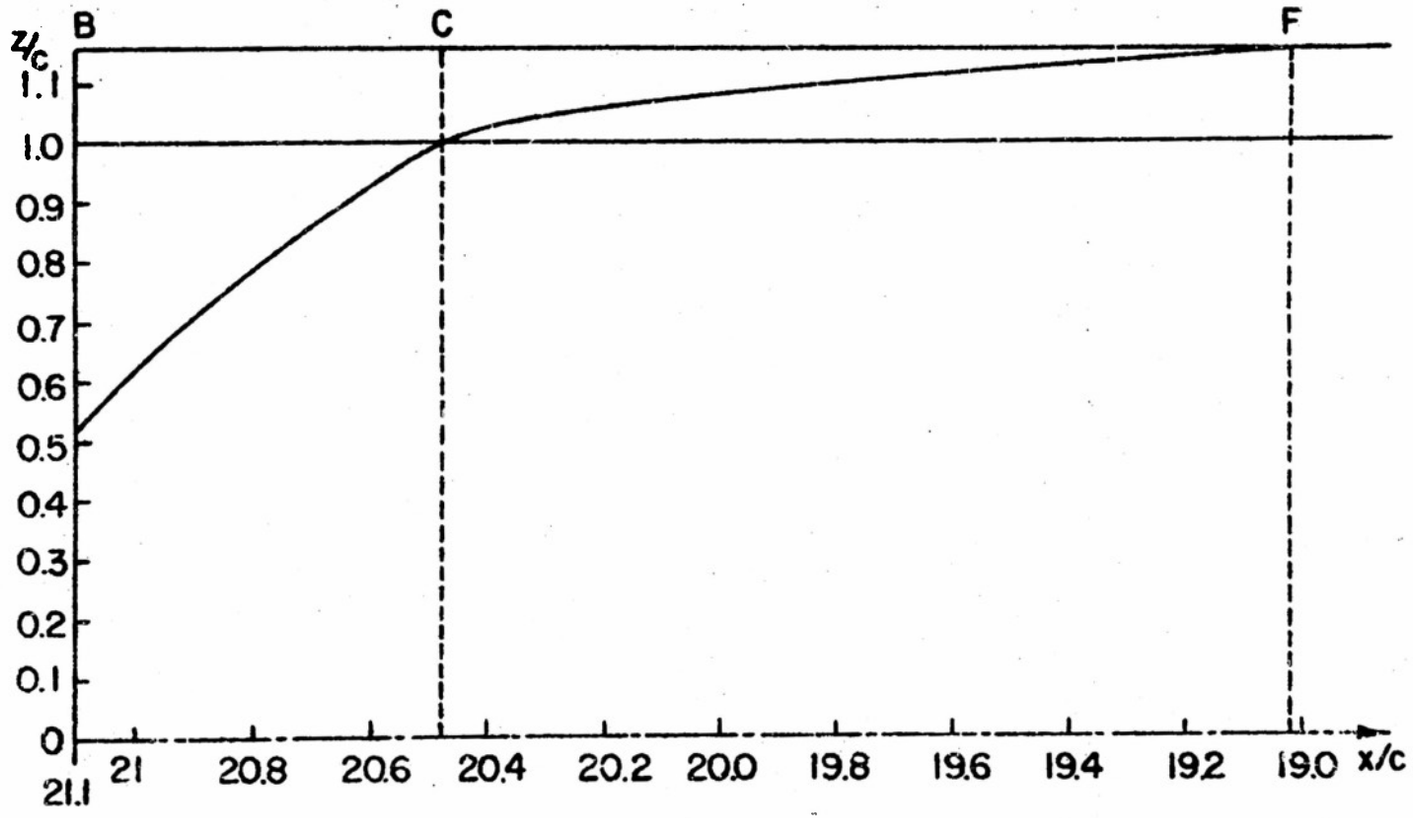

Fig. 12 The plastic region for 8WF40 section, $\ell/c = 21.1$

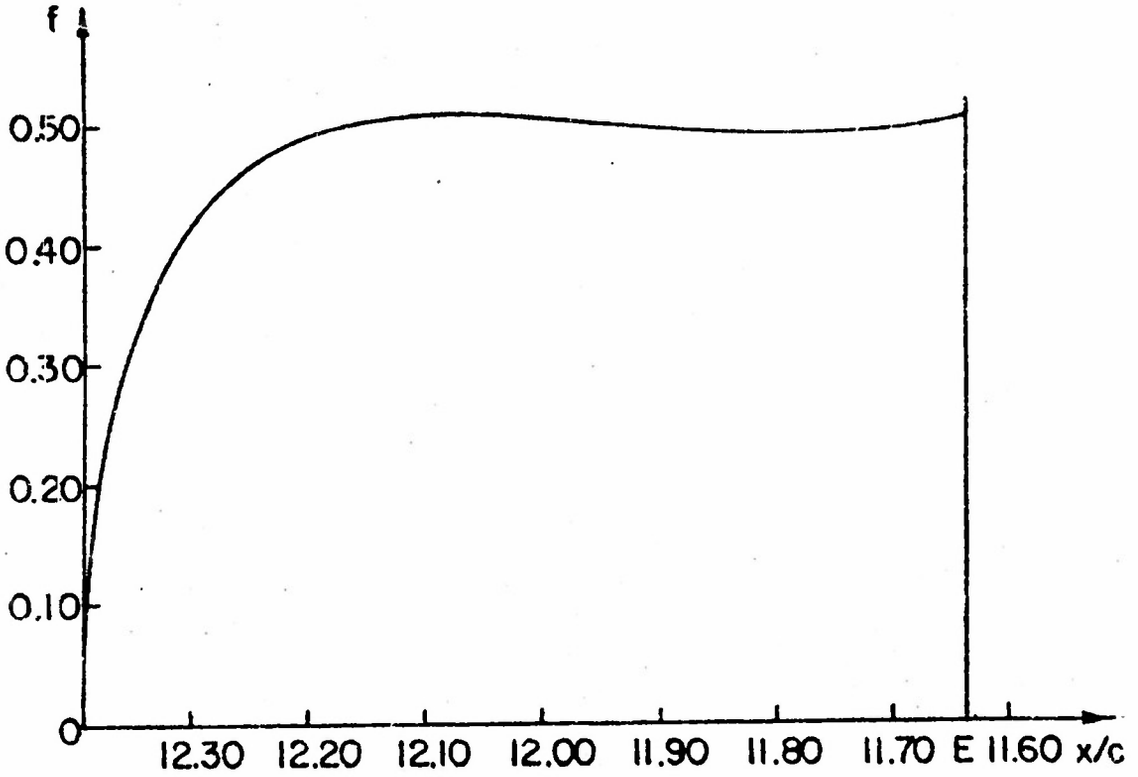

Fig. 13. The function f(x) for 8WF 40 section; $\ell/c = 12.5356$

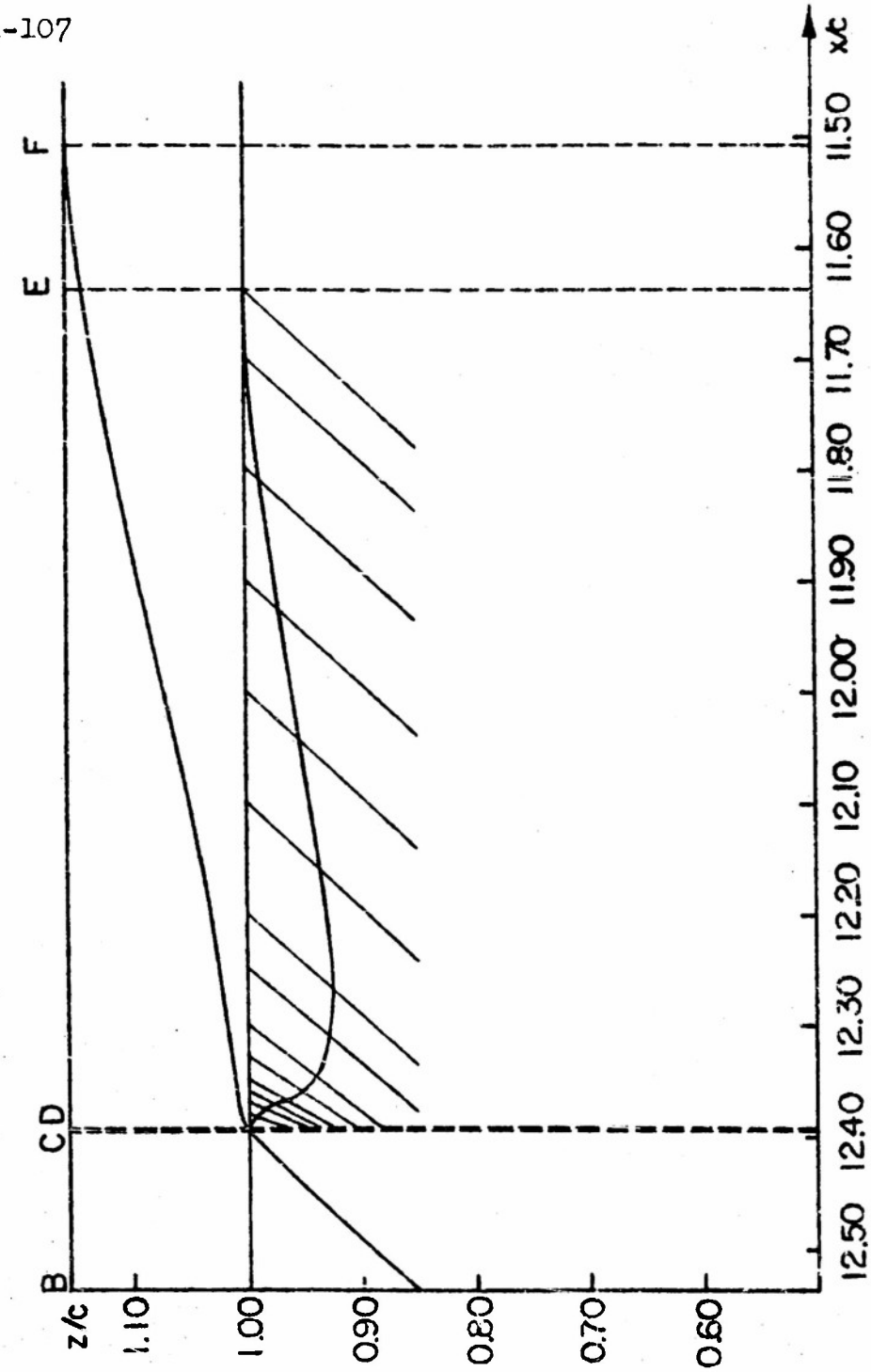

Fig. 14. The plastic regions for 8WF40 section; $\ell/c = 12.5356$

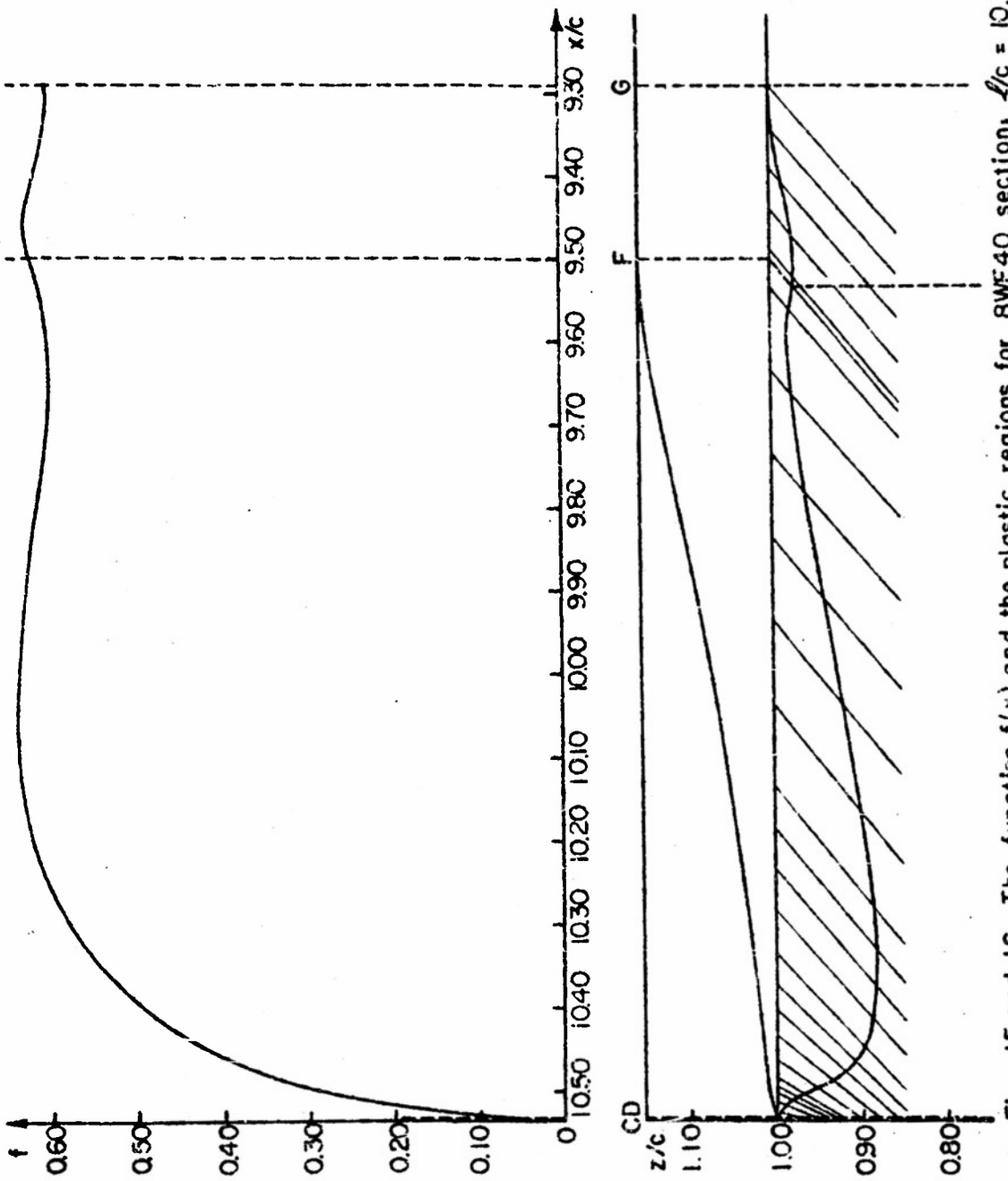

Figs. 15 and 16. The function f(x) and the plastic regions for 8WF40 section, $\ell/c = 10.53492$

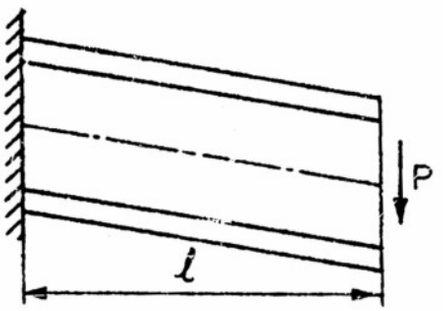

Fig. 17. Shear failure in the web

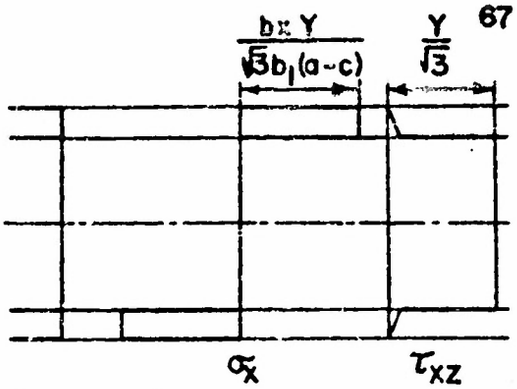

Fig. 18. The second type of stress field

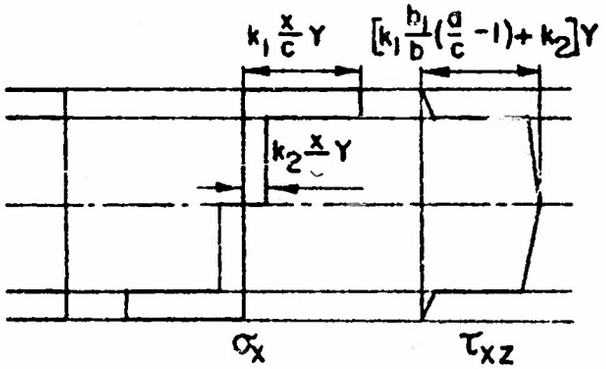

Fig. 19. The second type of stress field

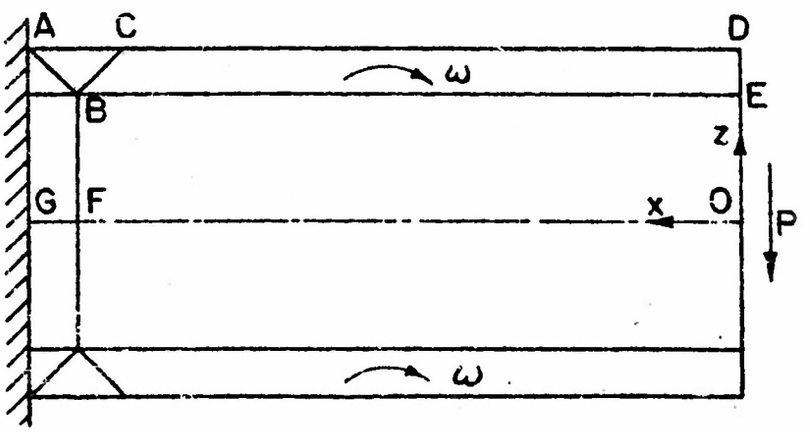

Fig. 20. The kinematically admissible velocity field

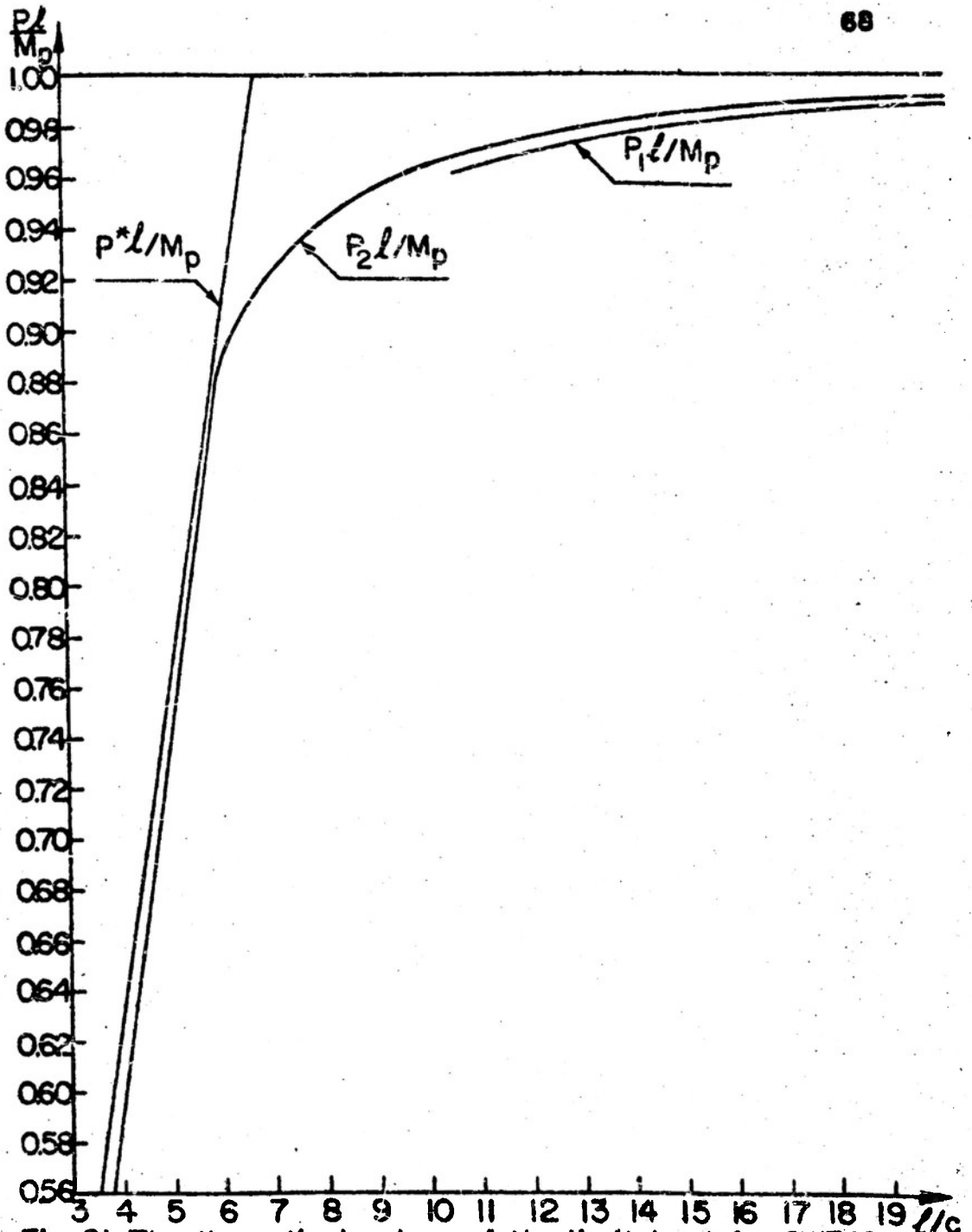

Fig. 21. The theoretical values of the limit load for 8WF40 section

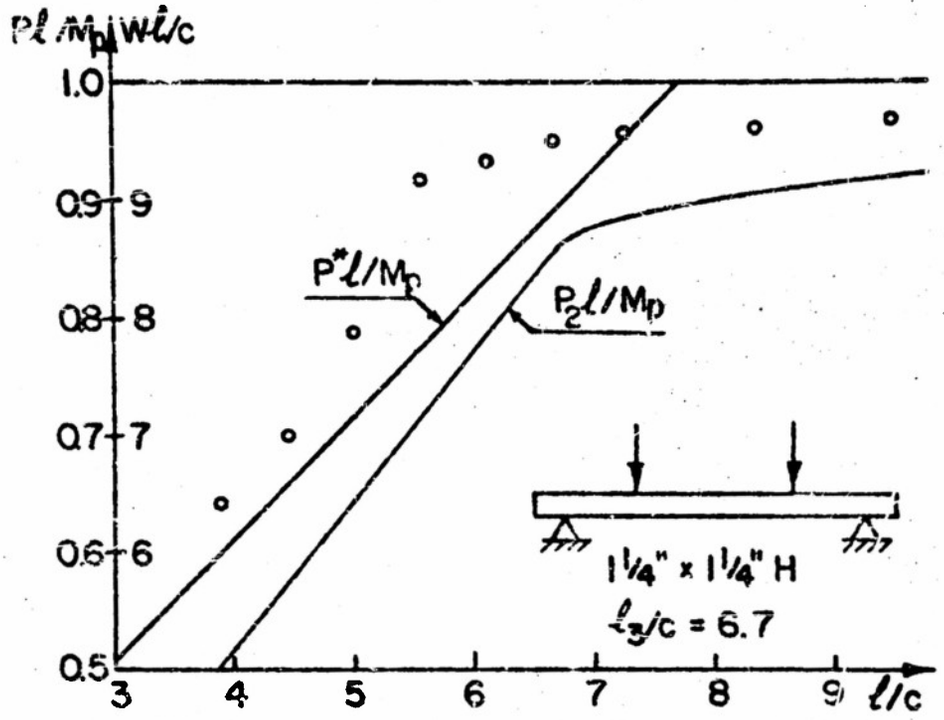

Fig. 22. The beam tests by Baker and Roderick [11]

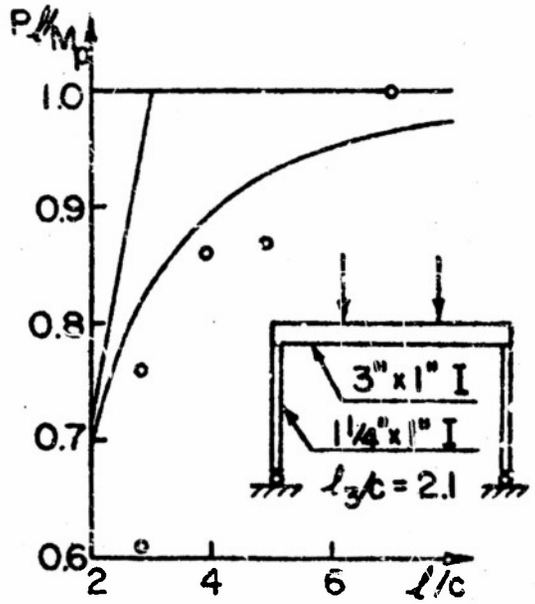

Fig. 24. The portal tests by Hendry [12]

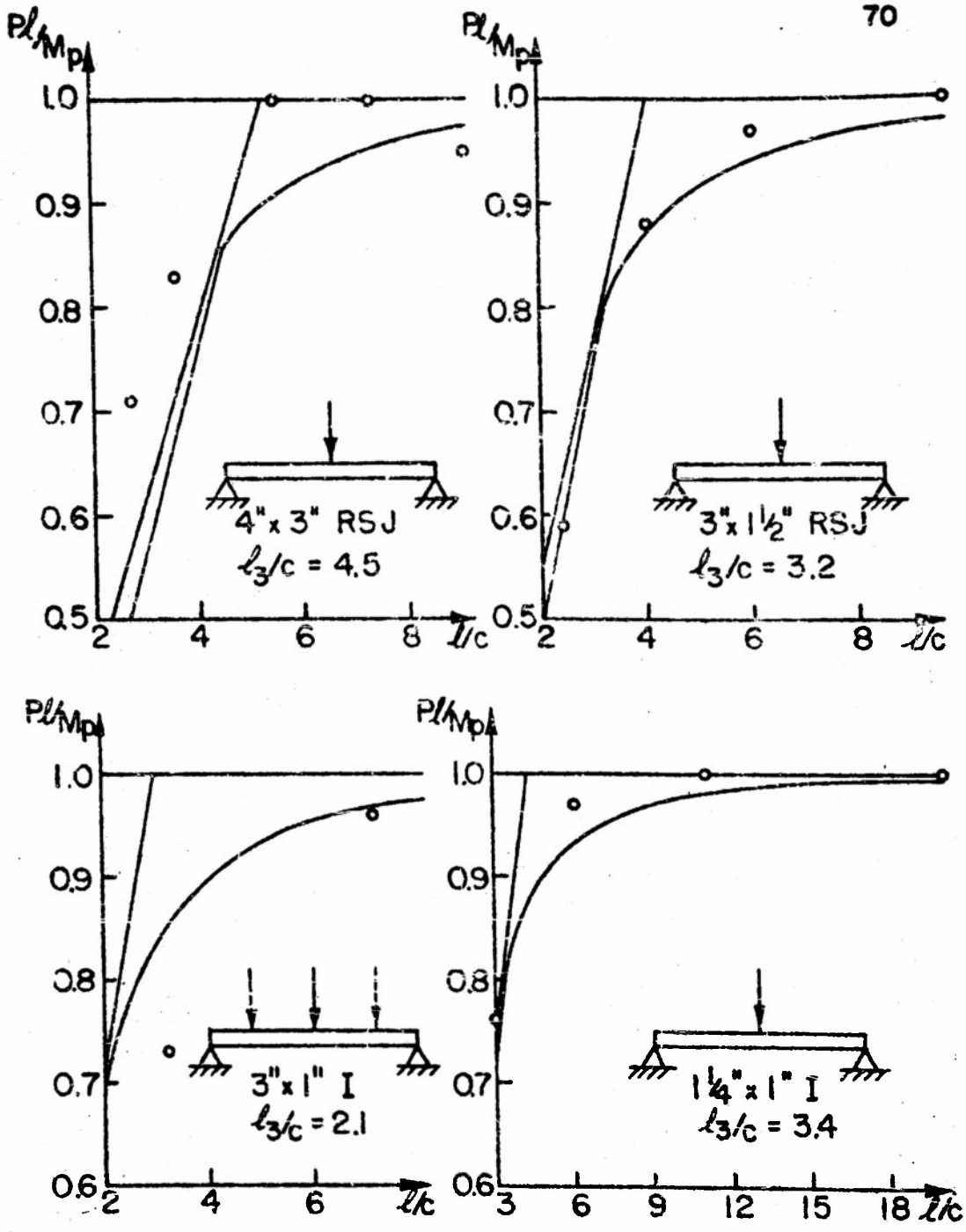

Fig. 23. The beam tests by Hendry [12]